This is a repository copy of *Globus pallidus dynamics reveal covert strategies for behavioral inhibition*.

White Rose Research Online URL for this paper:
http://eprints.whiterose.ac.uk/161807/

Version: Accepted Version

**Article:**

1 **Globus pallidus dynamics reveal covert strategies for behavioral inhibition.**

2 Bon-Mi Gu[1], Robert Schmidt[2], and Joshua D. Berke[1,3*]

3   1)  Department of Neurology, University of California, San Francisco, USA.

4   2)  Department of Psychology, University of Sheffield, UK.

5   3)  Department of Psychiatry; Neuroscience Graduate Program; Kavli Institute for Fundamental Neuroscience;
6        Weill Institute for Neurosciences, University of California, San Francisco, USA.

7       *Corresponding Author

8

9 **Abstract:**

10 Flexible behavior requires restraint of actions that are no longer appropriate. This behavioral

11 inhibition critically relies on frontal cortex - basal ganglia circuits. Within the basal ganglia the

12 globus pallidus pars externa (GPe), has been hypothesized to mediate selective proactive

13 inhibition: being prepared to stop a specific action, if needed. Here we investigate population

14 dynamics of rat GPe neurons during preparation-to-stop, stopping, and going. Rats selectively

15 engaged proactive inhibition towards specific actions, as shown by slowed reaction times (RTs).

16 Under proactive inhibition, GPe population activity occupied state-space locations farther from

17 the trajectory followed during normal movement initiation. Furthermore, the state-space

18 locations were predictive of distinct types of errors: failures-to-stop, failures-to-go, and incorrect

19 choices. Slowed RTs on correct proactive trials reflected starting bias towards the alternative

20 action, which was overcome before progressing towards action initiation. Our results

21 demonstrate that rats can exert cognitive control via strategic adjustments to their GPe network

22 state.

23

24 **Introduction.**

25       Our capacity for self-restraint is critical for adaptive behavior. Dysfunctions in behavioral

26 inhibition are involved in many human disorders, including drug addiction (Ersche *et al.* 2012). A

1

27  standard test of behavioral inhibition is the stop-signal task (Logan & Cowan 1984; Verbruggen

28  *et al.* 2019), in which subjects attempt to respond rapidly to a Go cue, but withhold responding if

29  the Go cue is quickly followed by a Stop cue. The stop-signal task has been invaluable for

30  revealing specific cortical-basal ganglia mechanisms involved in both movement initiation

31  ("Going"; e.g. Hanes & Schall 1996) and inhibition ("Stopping"; e.g. Aron & Poldrack 2006; Eagle

32  *et al.,* 2008). "Reactive" inhibition – making quick use of a Stop cue – appears to involve at least

33  two distinct mechanisms (Schmidt & Berke 2017): a rapid Pause process mediated via the

34  subthalamic nucleus (STN; Aron & Poldrack 2006; Schmidt *et al.,* 2013) followed by a Cancel

35  process achieved through pallidostriatal inhibition (Mallet *et al.,* 2016).

36      Behavioral inhibition can also be "proactive": restraint of actions, in advance of any Stop

37  cue. Proactive inhibition may be particularly relevant to human life (Aron 2011; Jahanshahi *et al.*

38  2015). Whereas reactive inhibition typically involves a global, transient arrest of actions and

39  thoughts (Wessel & Aron 2017), proactive inhibition can be selectively directed to a particular

40  action (Cai *et al.* 2011). A key behavioral signature of proactive inhibition is slowing of reaction

41  times (RTs) for that action, when the anticipated Stop cue does not actually occur (e.g.

42  Verbruggen & Logan 2008; Chikazoe *et al.* 2009; Zandbelt *et al.* 2012). This overt behavioral

43  signature presumably relies on covert shifts in information processing, yet the nature of these

44  shifts is unclear. In some studies fitting of models to behavioral data has suggested that slowed

45  RTs reflect raising of a decision "threshold" (Verbruggen & Logan 2009; Jahfari *et al.* 2012), but

46  other studies have found evidence for a slower rate of progression toward threshold instead

47  (Dunovan *et al.* 2015).

48      The neural circuit mechanisms by which proactive control is achieved are also not well

49  understood. It has been proposed that proactive inhibition critically depends on the basal

50  ganglia "indirect" pathway via GPe (Aron 2011; Jahanshahi *et al.,* 2015; Dunovan *et al.* 2015).

51  Yet direct support for this hypothesis is sparse (Majid *et al.* 2013). There have been few

52  electrophysiological studies of proactive inhibition at the level of individual neurons (Chen *et al.*

53  2010; Pouget *et al.* 2011; Hardung *et al.,* 2017; Yoshida *et al.* 2018), and to our knowledge none

54  in GPe. We therefore targeted GPe (often called simply GP in rodents) for investigating neural

55  mechanisms of proactive control.

56      We also wished to integrate a dynamical systems approach into the study of behavioral

57  inhibition, and the basal ganglia. Analysis of the collective dynamics of motor cortex neurons

58    has provided insights into various aspects of movement control, including how brain networks

59    may prepare actions without prematurely triggering them (Kaufman *et al.,* 2014), and the origins

60    of RT variability (Afshar *et al.* 2011). We demonstrate below that the analysis of GPe population

61    activity can reveal distinct covert strategies underlying overt manifestations of proactive control.

62

## Results

64    **Action initiation is slower when a stop cue is expected.**

65    We trained rats in a modified version of our stop-signal task (Figure 1A; Leventhal *et al.*

66    2012; Schmidt *et al.* 2013; Mallet *et al.* 2016). Freely-moving rats poked their noses into a hole

67    and maintained that position for a variable delay (500-1250 ms) before presentation of one of

68    two Go cues (1kHz or 4kHz tone), instructing leftward or rightward movements respectively into

69    an adjacent hole. If initiated rapidly (RT limit < 800 ms), correct movements triggered delivery of

70    a sugar pellet reward from a separate food hopper. On some trials the Go cue was quickly

71    followed by a Stop cue (white noise burst), indicating that the rat instead needed to maintain its

72    nose in the starting hole (for a total of 800 ms after Go cue onset) to trigger reward delivery. The

73    delay between Go and Stop cue onsets (100-250 ms) ensured that stopping was sometimes

74    successful and sometimes not. As expected, Failed Stop (error) trials had similar RTs to the

75    faster part of the Go trial RT distribution (Figure 1B). This is consistent with the basic "race"

76    conceptual model of reactive inhibition (Logan & Cowan 1984): failures-to-stop typically occur

77    when an underlying Go process evolves more quickly than average (Schmidt *et al.* 2013), and

78    thus wins the race against a separate Stop process.

79    To probe selective proactive inhibition we used a "Maybe-Stop versus No-Stop" approach

80    (Aron & Verbruggen 2008). The three possible starting holes were associated with different Stop

81    cue probabilities (Figure 1C): no possibility of Stop cue; 50% probability that a left Go cue (only)

82    will be followed by the Stop cue; or 50% probability that a right Go cue (only) will be followed by

83    the Stop cue. Our index of proactive inhibition was a preferential increase in RT for the Maybe-

84    Stop direction, compared to the No-Stop conditions. Among rats that began learning this task

85    variant, approximately half acquired clear proactive inhibition within 3 months of training (see

86    Methods), and were thus considered eligible for electrode implantation. Here we report

87  behavioral and neural results for 6 rats for which we were able to obtain high-quality GP

88  recordings as rats engaged proactive control.

89       We selected for further analysis those behavioral sessions (n=63) with a significant

90  proactive inhibition effect (i.e. longer RT when a Stop cue might occur; one-tail Wilcoxon rank

91  sum test, p<0.05) and distinct GP single units (n=376 neurons included). Prior work has shown

92  particular basal ganglia involvement in the control of contraversive orienting-type movements

93  (i.e. directed towards the opposite side; Carli *et al.* 1985; Isoda & Hikosaka 2008; Schmidt *et al.*

94  2013; Leventhal *et al.* 2014). We therefore focused on proactive control of movements

95  contraversive ("contra") to the recorded cell locations; e.g. we included a left GPe cell only if the

96  rat demonstrated proactive control for rightward movements during that recording session. For

97  included sessions, median RT for correct contra movements was 251ms when the Stop cue

98  could not occur (No-Stop), and 385ms when the Stop cue could occur (Maybe-Stop) but did not.

99  Results from all sessions, and from individual animals, are shown in Figure 1 - figure

100 supplement 1.

101       RT slowing due to proactive inhibition was highly selective to the Maybe-Stop direction

102 (Figure 1D; Figure 1 - figure supplement 1; for Maybe-Stop-Contra trials without a Stop cue,

103 median ipsiversive ("ipsi") RT was unslowed at 264ms). The Maybe-Stop condition was also

104 associated with an increase in errors (Figure 1D), in particular not responding quickly enough to

105 the Go cue that might be followed by Stop (RT limit error; RT > 800ms) and making the wrong

106 choice (incorrect action selection). These error types are examined further below.

107

108 **GP firing rate changes related to movement onset and proactive inhibition.**

109       We recorded individual neurons (n=376) from a wide range of GP locations (Figure 2-

110 figure supplement 1A). As expected from prior studies (DeLong 1971; Brotchie et al.1991;

111 Gardiner & Kitai 1992; Turner & Anderson 1997; Arkadir *et al.* 2004; Gage *et al.* 2010; Shin &

112 Sommer 2010; Schmidt *et al.* 2013; Yoshida & Tanaka 2016; Mallet *et al.* 2016) GP neurons

113 were tonically-active (mean session-wide firing rate, 28Hz) with diverse, complex changes in

114 firing patterns during task performance (Figure 2A). The majority of GP cells showed strongest

115 firing rate changes (increases or decreases) when activity was aligned relative to movement

116 onset, rather than to the Go or Stop cues (Figure 2C,D; see also Figure 2-figure supplement 1B

117   for ipsi movement trials). Individual neurons showed greater changes for either contra or ipsi

118   movements (Figure 2A,B), but these were about equally represented in the overall population

119   (Figure 2B,E), and the average GP activity was similar for the two movement directions (at least

120   until the movement was already underway; Figure 2B).

121       We next examined how the activity of individual GP neurons is affected by proactive

122   inhibition. As rats waited for the (unpredictably-timed) Go cue, average firing was similar

123   between Maybe-Stop and No-Stop conditions (Figure 2F), regardless of whether we examined

124   cells that predominantly increase or decrease activity during movements (Figure 2-figure

125   supplement 1C). We hypothesized that this average activity obscures a sizable GP

126   subpopulation that consistently and persistently "encodes" proactive control as rats wait. To

127   search for this putative subpopulation we used a screening approach (similar to our prior work

128   on reactive stopping; Schmidt *et al.* 2013, Mallet *et al.* 2016), comparing the Maybe-Stop-contra

129   and No-Stop conditions. We did find that the fraction of GP cells that fired differently between

130   these conditions was slightly greater than expected by chance (Figure 2F), consistent with GP

131   involvement in proactive control. However, contrary to our hypothesis, we were not able to

132   identify a clear subgroup of individual neurons that strongly and persistently distinguished

133   between conditions (Fig. 2G). Rather, proactive control was associated with altered activity in

134   different subsets of GP neurons at various brief moments before the Go cue (Fig. S2D).

135

136   **Population trajectories during movement selection and initiation**.

137       We next hypothesized that these GP firing rate differences, though subtle and diverse at

138   the single-cell level, are coordinated to produce clear, interpretable changes in population

139   dynamics. To observe these dynamics we began by reducing the dimensionality of population

140   activity (Cunningham & Yu 2014), using principal component analysis (PCA). For each neuron

141   we included normalized, averaged firing rates for a 500ms epoch around movement onset

142   (separately for contra and ipsi movements; Figure. 3A). We used the first 10 principal

143   components (PCs; Figure 3-figure supplement 1A) to define a 10-dimensional state-space, with

144   GP population activity represented as a single point in this space. For visualization we display

145   the first 3 PCs (which together account for 71% of total population variance; Figure 3B),

146   although statistical analyses used all 10 PCs.

147    Within state space, population activity was very similar for contra and ipsi movements at

148    the Go cue (Figure 3C), and initially evolved in a common direction before progressively

149    separating into distinct trajectories (Video 1). We used the common direction to define an

150    "*Initiation Axis*", scaled between 0 (mean location at Go cue) and 1 (mean location at movement

151    onset, Center Out). This allows us to quantify progression towards (or away from) movement

152    onset. We used the difference between trajectories to define a "*Selection Axis*", scaled between

153    -1 (mean of the ipsi trajectory) and +1 (mean of the contra trajectory). This allows us to quantify

154    bias toward one movement direction or the other. Along both Initiation and Selection axes,

155    change was not dominated by a small proportion of GP neurons. Instead, there were smaller

156    contributions from many individual cells located throughout GP (Figure 3-figure supplement

157    1AC-E).

158

159    **Failed stops reflect earlier evolution of GP activity.**

160    We then considered how GP population activity is evolving when Stop cues occur. As

161    noted above, standard race models of reactive stopping (Logan & Cowan 1984), together with

162    prior data (Schmidt *et al.* 2013), suggest that failures-to-Stop occur when an underlying Go

163    process evolves more quickly than average, and thus the Stop cue arrives too late. GP

164    population activity was consistent with these ideas (Figure 3D-F). On successful-Stop trials GP

165    activity showed little or no movement before the Stop cue. By contrast, on failed-Stop trials GP

166    activity was in a significantly different state by the time of the Stop cue, having already evolved a

167    substantial distance along the Initiation Axis (Figure 3D; includes both contra- and ipsi-cued

168    trials). Thus, our observations of neural dynamics support hypothesized internal dynamics that

169    determine whether we can react to new information, or are already committed to a course of

170    action.

171

172    **When Stop cues may occur, GP activity starts farther from movement initiation.**

173    Conceptually, the slowing of RT with proactive inhibition could reflect any of several

174    distinct underlying changes (Figure 4A), that would manifest in GP dynamics in different ways. If

175    slowing involves mechanisms "downstream" of GP, we might observe no change in the GP

176    population trajectory when aligned on the Go cue (*hypothesis 1).* Alternatively, the GP might be

177 in a different state at the time the Go cue arrives. In particular, GP activity might start farther
178 away from "threshold" (in dynamical terms, farther from a subspace associated with movement
179 initiation), and thus take longer to get there *(hypothesis 2).* Finally, proactive inhibition might
180 cause GP activity to evolve differently *after* Go cue onset. Various, non-mutually-exclusive
181 possibilities include a delayed start *(hypothesis 3)*, slower progress along the same trajectory
182 *(hypothesis 4),* and/or a threshold that is shifted further away from the starting point *(hypothesis*
183 *5)*. Of note, only hypothesis 2 predicts a change in the trajectory start location at the time of the
184 Go cue (Figure 4A).

185    We compared GP population activity between Maybe-Stop and No-Stop conditions,
186 immediately before the Go cue (-100ms - 0ms; including all trial subtypes). When proactive
187 inhibition was engaged, GP activity occupied a significantly shifted location within state-space
188 (Figure 4B,C). When examined along the Initiation axis (Fig. 4C), the direction of this shift was
189 consistent with a longer trajectory required for movements to begin (*hypothesis 2)*. In other
190 words, the brain can restrain actions by placing key circuits into a state from which actions are
191 slower to initiate.

192

193 **Distinct state-space positions predict distinct types of errors.**

194    Proactive inhibition of contra movements also produced a significant shift along the
195 Selection axis before the Go cue, in the direction associated with ipsi movements (Figure 4C).
196 This suggests a preparatory bias against contra movements, when the contra-instructing Go cue
197 may be followed by a Stop cue. To examine how starting position affects behavioral outcome,
198 we examined how state-space location at the Go cue varies with distinct types of errors (Figure
199 4D). Failures to respond quickly enough to the Go cue (RT limit errors) were associated with
200 starting farther away on the Initiation Axis (Figure 4E). By contrast, incorrect choices (ipsi
201 movements despite contra cue) were associated with starting closer to movement initiation,
202 together with a more-ipsiversive position on the Selection axis at Go cue (Figure 4E; Video 2).
203 Thus, even while the animals are holding still, waiting for the Go cue, GP networks show
204 distinctly-biased internal states that predict distinct subsequent behavioral outcomes.

205

206 **Overcoming a selection bias delays movement initiation.**

207  The starting ipsiversive bias on the Selection axis when contra actions might have to be

208  cancelled can be overcome, as even on contra Maybe-Stop trials the rats usually made the

209  correct choice. To examine how this occurs we compared neural trajectories for correct, contra

210  Maybe-Stop and No-Stop trials (Figure 5A; only correct trials without Stop cues are included).

211  Just before the Go cue on Maybe-Stop trials, rats showed no difference on the Initiation Axis but

212  were significantly shifted on the Selection axis, in the ipsiversive direction (Figure 5A,B). After

213  the Go Cue, movement on the Initiation axis was delayed compared to No-Stop trials, but

214  movement on the Selection Axis occurred earlier (Figure 5C; Video 3). Thus, on correctly-

215  performed Maybe-Stop trials the GP network engaged a dynamical sequence that was not

216  observed on No-Stop trials: they first overcame a proactive bias towards the alternative action,

217  before proceeding to initiate the action that had been cued.

218  Together our results indicate that, when faced with the challenging Maybe-Stop condition,

219  rats adopt multiple, distinct, covert strategies. They can position neural activity farther from

220  movement onset (on the Initiation Axis), but this produces limited hold violations – essentially

221  making this a bet that the Stop cue will in fact occur. Alternatively, they can bias neural activity

222  in the ipsi direction (on the Selection Axis). This delays contra choices, but also increases the

223  rate of incorrect ipsi choices.

224

225  **Slower RTs can arise through multiple dynamic mechanisms.**

226  We considered the possibility that this apparent "strategy" for proactive inhibition simply

227  reflects the slower RT. In other words, is the distinct trajectory seen for correct Maybe-Stop trials

228  also seen for slower No-Stop trials? Our data indicate that this is not the case. Comparing

229  Maybe-Stop trials with No-Stop trials with the same RT (RT-matching) again showed different

230  positions on the Selection Axis at Go cue (Figure 5 - figure supplement 1). This difference was

231  not seen when comparing slower and faster RTs within the No-Stop condition (Figure 5D,E).

232  Rather, spontaneously-slower RTs appeared to arise through slower evolution along both

233  Initiation and Selection Axes simultaneously (Figure 5F). Furthermore, on Maybe-Stop trials

234  movement along the Selection axis overshot the level reached on No-Stop trials, as if

235  overcompensating for the initial bias on this axis (Figure 5A, Figure 5 - figure supplement 2).

236  This overshoot was not seen for spontaneously-slower No-Stop trials (Figure 5 - figure

237  supplement 2). We conclude that variation in RT reflects multiple dynamic processes within

238   basal ganglia circuits, with slowing due to proactive inhibition involving distinct internal control
239   mechanisms to spontaneous RT variation.

240        Although reducing the dimensionality of data can be very useful for visualizing
241   trajectories through state-space, we wished to ensure that our conclusions are not distorted by
242   this procedure. We therefore repeated key analyses within the full 376-dimensional state space.
243   Defining Initiation and Selection Axes in the same way as before, but without the PCA step,
244   produced essentially identical trajectory differences between conditions (Figure 6).

245

246


## Discussion.

248        Stop-signal tasks are widely-used to test cognitive control (Lipszyc & Schachar 2010),
249   with proactive inhibition considered especially reliant on top-down, effortful, resource-demanding
250   processes (Jahanshahi *et al.* 2015). Yet there have been extended debates about which
251   psychological and neural mechanisms support proactive control (Verbruggen & Logan 2009;
252   Chatham *et al.* 2012; Aron *et al.* 2014; Leunissen *et al.* 2016). We have demonstrated here that
253   a key behavioral signature of proactive control – selective slowing of RTs when a Stop signal is
254   expected - can arise through multiple covert strategies. These are visible as changes to the
255   dynamic state of GPe by the time of Go cue presentation, and include a bias towards an
256   alternative action, and/or starting further from the "point-of-no-return" in action initiation.

257        Which internal strategies are employed for proactive inhibition is likely influenced by the
258   specific experimental conditions (Mayse *et al.* 2014; Yoshida *et al.* 2018). For example, we used
259   a brief limited hold period (800ms) to encourage subjects to respond rapidly to the Go cue rather
260   than waiting to see if the Stop cue is presented. This time pressure may have led rats to
261   sometimes make guesses as to which cues will be presented, and position their neural state
262   accordingly. We also used a task design with asymmetric (ipsi/contra) stop probabilities, to
263   probe the selectivity of proactive inhibition (Aron & Verbruggen 2008). Motivational aspects are
264   known to be important in proactive inhibition (Meyer & Bucci 2016): the ipsi bias we observed on
265   the Selection axis on Maybe-Stop (contra) trials may partly reflect asymmetric reward
266   expectancy (Kawagoe *et al.* 1998), simply because ipsi movements are more consistently
267   rewarded from that state. Unlike human subjects, we cannot verbally instruct rats to perform the

268 task in a certain way (although human cognitive strategies do not always follow experimenter

269 intentions either). It might seem simpler, and less error-prone, for the rats to just select from the

270 slower portion of their regular RT distribution. We suggest that they are unable to consistently

271 do so, given the high spontaneous variability in RTs. The degree to which specific neural

272 strategies are employed may also vary between rats; we found some preliminary evidence for

273 this (Figure 4 -figure supplement 1), though investigating this further would require more animals

274 and more recorded cells in each animal.

275 The term "proactive" or "cognitive" control has been used to refer both to stop-signal

276 tasks like this one, in which subjects are cued about the upcoming stop probability (e.g. Cai *et*

277 al. 2011; Jahfari *et* al. 2012; Zandbelt *et al.* 2012), and also to uncued behavioral adjustments

278 that subjects make after each trial (e.g. longer RTs following trials in which Stop cues occurred;

279 e.g. Chen *et al.* 2010; Pouget et al. 2011; Mayse *et al.* 2014). Although not the focus of this

280 study, our rats did slow down slightly on average after Stop trials or errors (Figure 4 -figure

281 supplement 2A). This slowing was associated with a modest shift on the Initiation Axis in the

282 same, movement-opposed direction as in our main results (Figure 4 -figure supplement 2B), but

283 this effect did not reach significance. Thus both behavioral and neural data suggest that the

284 cued component of proactive inhibition was substantially greater than post-trial adjustments

285 under our particular task conditions.

286 Our ability to reveal distinct strategies for proactive inhibition relies on a dynamical

287 systems approach with single-cell resolution. This method may be especially important for

288 deciphering structures like GP, where projection neurons show continuous, diverse activity

289 patterns. As intermingled GP neurons increased and decreased firing at each moment, the

290 resulting network state changes would likely be undetected using aggregate measures such as

291 photometry or fMRI. Speculatively, we suggest that an enhanced ability to make subtle

292 adjustments to dynamical state may be part of the reason why GP projection neurons show high

293 spontaneous activity, in contrast to (for example) the near-silence of most striatal projection

294 neurons, most of the time.

295 Prior examinations of motor/premotor cortical dynamics during reaching movements in

296 non-human primates have demonstrated distinct neural dimensions for movement preparation

297 and execution ("*What*" to do) and movement triggering ("*When*" to do it) (Elsayed *et al.,* 2016;

298 Kaufman *et al.* 2016). Our Selection and Initiation axes are analogous, although our task lacks

299  an explicit preparation epoch and has only two action choices (left vs. right). One notable

300  difference in the non-human primate studies is that movement preparation occurred in distinct,

301  orthogonal dimensions to movement execution, whereas we saw preparatory "bias" along the

302  same Selection axis that differentiated ipsi and contra trajectories during movement itself.

303  Nonetheless, our observation that on correct Maybe-Stop trials, GP state evolved first along the

304  Selection axis is consistent with evidence that movement preparation and movement initiation

305  can be independent processes (Haith *et al.* 2016; Thura & Cisek 2017), and that these can be

306  differentially modulated by the basal ganglia and dopamine (Leventhal *et al.* 2014; Manohar *et*

307  *al.* 2015). It also appears consistent with recent observations that, following an unexpected late

308  change in target location, preparation dimensions are rapidly re-engaged (Ames *et al.* 2019).

309       The distinction between *What* and *When* dimensions is not readily compatible with

310  sequential-sampling mathematical models of decision-making (Smith & Ratcliff 2004; Brown &

311  Heathcote 2008; Noorani & Carpenter 2016), which typically assume that RTs (*When*) directly

312  reflect sufficient accumulation of evidence for a particular choice (*What*). Furthermore, when

313  sensory cues are unambiguous the selection process appears to be much faster than standard

314  RTs (Stanford *et al.* 2010; Haith *et al.* 2016). Why RTs are typically so much slower and more

315  variable than required for sensory processing or action selection is not fully clear, but this extra

316  time provides opportunity for impulsive or inappropriate responses to be overruled, to increase

317  behavioral flexibility.

318       The GPe is well positioned to contribute to such behavioral control. GPe has bidirectional

319  connections with the subthalamic nucleus, a key component of the "hyperdirect" pathway from

320  frontal cortex that slows decision-making under conditions of conflict (Cavanagh *et al.* 2011).

321  GPe itself is the target of the "indirect" (striatopallidal) pathway, believed to discourage action

322  initiation ("NoGo"; Yoshida & Tanaka 2009; Kravitz *et al.* 2010), possibly due to pessimistic

323  predictions of reward (Collins & Frank 2014; Kim *et al.* 2017). In standard, firing rate-based

324  models of basal ganglia function, GPe activity restrains actions by preventing pauses in the

325  firing of basal ganglia output, that are in turn required to disinhibit movement-related activity in

326  the brainstem and elsewhere (Chevalier & Deniau 1990; Roseberry *et al.* 2016).

327       However, it is well-recognized that this model is too simple (Gurney *et al.* 2001; Klaus *et*

328  *al.* 2019), and it does not account for the complex activity patterns within GPe that we and

329  others have observed. For example, a straightforward application of the rate model might predict

330     a systematic decrease in GPe firing rate with proactive inhibition, but we did not observe this

331     (Figure 2), with the possible exception of trials with RT limit errors (Figure 2 -figure supplement

332     1). Based on the current results, examining dimension-reduced population dynamics is a

333     promising alternative approach for deciphering how subtle modulations in the firing of many

334     basal ganglia neurons are coordinated to achieve behavioral functions.

335     At the same time, our study has several noteworthy limitations. Our reduction of complex

336     dynamics to movement along Initiation and Selection axes is obviously a simplification. We did

337     not record large populations of neurons simultaneously, which precludes effective analysis of

338     neural dynamics on individual trials (Afshar *et al.* 2011). We did not classify GPe neurons by

339     projection target (Mallet *et al.* 2012; Abecassis *et al.* 2020) largely because we did not

340     consistently record sleep data to enable that classification (Mallet *et al.* 2016). We do not yet

341     know the extent to which these population dynamics are shared with upstream (e.g. striatum)

342     and downstream (e.g. substantia nigra pars reticulata) structures, which will be essential for

343     elucidating how these dynamic changes actually influence behavior. Finally, we have not yet

344     determined how the population dynamics reported here relate (if at all) to oscillatory dynamics

345     reported in cortical-basal ganglia circuits during movement suppression (Swann *et al.*

346     2009; Cavanagh *et al.* 2011; Leventhal *et al.* 2012) and in pathological states such as

347     Parkinson's Disease (Hammond *et al.* 2007). These are all worthy subjects for future

348     investigation.

349

350

351

352 **Key Resources:** Rat (adult, male, Long-Evans, bred in-house).

353 **Methods.**

354     All animal experiments were approved by the University of California, San Francisco
355 Committee for the Use and Care of Animals. Adult male Long-Evans rats were housed on a
356 12h/12h reverse light-dark cycle, with training and testing performed during the dark phase.

357 **Behavior.** Operant chambers (Med Associates, Fairfax VT) had five nose-poke holes on one
358 wall, a food dispenser on the opposite wall, and a speaker located above the food port. The
359 basic rat stop signal task has been previously described (Leventhal *et al.* 2012.; Mallet *et al.*,
360 2016, Schmidt *et al.*, 2013). At the start of each trial, one of the 3 more-central ports was
361 illuminated ('Light On') indicating that the rat should poke in that port ('Center In') and wait. After
362 a variable delay (500-1250ms), a higher (4 kHz) or lower (1kHz) pitch tone was presented for
363 50ms ('Go Cue'), instructing a move to the adjacent port on the left or right side respectively. In
364 Go trials (those without a Stop cue) if the rat left the initial center port ('Center Out') within
365 800ms of Go cue onset, and then moved to the correct side port ('Side In') within 500ms, a
366 sugar pellet reward was delivered to the food dispenser with an audible click. As the rat left the
367 center port, the center port light was turned off and both side port lights turned on. On Stop
368 trials, the Go cue was followed by a Stop cue (white noise, 125ms) with a short delay (the stop-
369 signal delay, SSD). The SSD was randomly selected on each trial within a range (uniform
370 distribution) of 100-200ms (4 rats) or 100-250ms (2 rats). Stop trials were rewarded if the rat
371 maintained its nose continuously within the start hole for a total of 800ms after Go cue onset.
372 Stop trials in which the rat initiated movement before the Stop cue began were converted into
373 Go trials (i.e. no Stop cue was presented). Failed-Stop trials with RT > 500ms were excluded
374 from electrophysiological analyses, since these were presumed to reflect trials for which rats
375 successfully responded to the Stop cue, but then failed to maintain holding until reward delivery
376 (see Leventhal *et al.* 2012; Schmidt *et al.* 2013; Mayse *et al.* 2014). Inter-trial intervals were
377 randomly selected between 5-7s. For included sessions, the median number of Go trials was
378 266 (range, 167-361) and the median number of Stop trials was 57 (range, 27-95).

379     To vary proactive inhibition, we changed the Stop cue probabilities between starting
380 holes (as shown in Figure 1). The spatial mapping of probabilities was constant for each rat
381 across sessions, but varied between rats. Within each session, the same start hole (and thus
382 proactive condition) was repeated for 10-15 trials at a time. After ~3 months of training, rats

383 showing consistent reaction time differences between Maybe-Stop and No-Stop conditions were

384 eligible for electrode implantation.

385 **Electrophysiology.** We report GP data from 6 rats (all animals in which we successfully

386 recorded GP neurons during contraversive proactive inhibition). Each rat was implanted with 15

387 tetrodes (configured as independently-driveable bundles of 2-3 tetrodes, each within a polyimide

388 tube with outer radius 140μm), bilaterally targeting GP and substantia nigra reticulata (SNr).

389 During task performance, wide-band (0.1-9000Hz) electrophysiological data were recorded with

390 a sampling rate of 30000/s using an Intan RHD2000 recording system (Intan Technologies). All

391 signals were initially referenced to a skull screw (tip-flattened) on the midline 1 mm posterior to

392 lambda. For spike detection we re-referenced to an electrode common average, and wavelet-

393 filtered (Wiltschko *et al.* 2008) before thresholding. For spike sorting we performed automatic

394 clustering units using MountainSort (Chung *et al.* 2017) followed by manual curation of

395 clusters. Tetrodes were usually moved by 159μm every 2-3 sessions. To avoid duplicate

396 neurons we did not include data from the same tetrode across multiple sessions unless the

397 tetrode had been moved by > 100μm between those sessions. Based on waveform and firing

398 properties we further excluded an additional 25 units that appeared to be duplicates even

399 though the tetrode had been moved. After recording was complete, we anesthetized rats and

400 made small marker lesions by applying 10μA current for 20s for one or two wires of each

401 tetrode. After perfusing the rats and slicing (at 40μm) tissue sections were stained with cresyl

402 violet and compared to the nearest atlas section (Paxinos & Watson 2006).

403 **Data analysis.** Smoothed firing rates were obtained convolving each spike time with a

404 Gaussian kernel (30ms SD). Firing rates were normalized (*Z*-scored) using the neuron's

405 session-wide mean and SD. Normalized average time series for contra and ipsi actions (500ms

406 each, around Center Out) were concatenated and used to construct a population activity matrix

407 **R** = TC by N, with T = 251 (timepoints, at 2ms intervals), C=2 (ipsi/contra conditions), and

408 N=376 (the number of neurons). We subtracted the mean of each of the N columns to make

409 data zero-centered, then performed principal components analysis (PCA) over matrix **R** using

410 the MATLAB 'svd' function. Using the right singular vectors (*W*), we can calculate the PC scores

411 (*S*) as $S=\mathbf{R}W$. For example, the first column of *S* contains the first principal component (PC1)

412 over time, and the first column of *W* contains the weights for each of the N units for PC1. We

413 used the first 10 PCs for analysis, and the Euclidean distance between conditions was

414 compared in this 10-D space. The projections onto the Initiation or Selection Axes were

415    calculated as the dot product of the state space position vector and the axis vector. State-space

416    positions around the Go cue (or Stop cue) were calculated using the set of weights $W$ to project

417    the Go cue–aligned (or Stop cue-aligned) firing rates into the 10-D PC space. In other words,

418    each neuron has a weight for each PC, and we calculate a net population position along each

419    PC by multiplying each neuron's instantaneous firing rate by its weight, and summing across all

420    neurons.

421          To test if whether state-space positions for two conditions (e.g. Successful- and Failed-

422    Stops) are significantly separated, we ran permutation tests by randomly shuffling the trial

423    conditions for each neuron (10000 shuffles for each test). Then, the distance in the population

424    state space at each time point was reconstructed using the firing rate differences between the

425    shuffled trial averages for each condition. For example, if the mean FR of a unit (n) in surrogate

426    Failed Stop trials (c1) and surrogate Successful Stop trials (c2) at Stop cue time (t) is $r_{(t,c1,n)}$

427    and $r_{(t,c2,n)}$, respectively, the difference between two conditions in k-dimension, $\Delta x_{(t,k)}$ is:

$$\Delta x_{(t,k)} = \sum_{n=1}^{N} \left( r_{(t,c1,n)} - r_{(t,c2,n)} \right) \times w_{(n,k)}$$

428    Repeated shuffling produces a surrogate data distribution for differences at each time point, and

429    the original difference between conditions is compared to this distribution to determine statistical

430    significance.

431

432

433

438 **Data and Code Availability.** The neurophysiology data and analysis code used in this

439 study are available from the to the public website Figshare:

440 https://figshare.com/articles/Globus_pallidus_dynamics_reveal_covert_strategies_for_behaviora

441 l_inhibition/12367541

442

**Figure Legends.**

444 **Figure 1. Reactive and Proactive Behavioral Inhibition**. **A**. Left, operant box configuration;
445 right, event sequence for Go and Stop trials. RT, reaction time; MT, movement time; SSD, stop-
446 signal delay; Reward, delivery of a sugar pellet to the food port. **B**. Left, distributions of Go and
447 Failed-Stop RTs (on Maybe-Stop trials; shading, S.E.M. across n = 63 sessions). Failed-Stop
448 RTs are similar to the faster part of the Go RT distribution, consistent with the "race" model in
449 which a relatively-fast Go process produces failures to stop. The tail of the Failed-Stop
450 distribution (RT > 500ms) is presumed to reflect trials for which rats successfully responded to
451 the Stop cue, but then failed to maintain holding until reward delivery (see Leventhal *et al.* 2012;
452 Schmidt *et al.* 2013; Mayse *et al.* 2014). Right, proportions of failed and successful Stop trials
453 after Contra and Ipsi Go cues. Error bars, S.E.M. across n=63 sessions. **C**. Trial start location
454 indicates stop probabilities (locations counterbalanced across rats). In this example
455 configuration recording from left GP, starting from the middle hole indicates the Maybe-stop
456 Contra condition: Go cues instructing rightward movements might be followed by a Stop cue,
457 but Go cues instructing leftward movements will not. **D**. Proactive inhibition causes selective RT
458 slowing for the Maybe-Stop direction (two-tail Wilcoxon signed rank tests on median RT for each
459 session: contra cues in Maybe-Stop-contra versus No-Stop, z=7.7, p=1.15×10$^{-14}$; ipsi cues in
460 Maybe-Stop-contra versus No-Stop, p=0.32). Additionally, under selective proactive inhibition
461 rats were more likely to fail to respond quickly enough (RT limit errors; Wilcoxon signed rank
462 tests, z=7.2, p=5.41×10$^{-13}$) and to select the wrong choice (uncued action direction; Wilcoxon
463 signed rank tests, z=7.0, p=2.59×10$^{-12}$). Error bars, S.E.M. across n=63 sessions. Only trials
464 without a Stop cue are included here. *RT limit error* = Nose remained in Center port for >800ms
465 after Go cue onset; *MT limit error* = movement time between Center Out and Side port entry >
466 500ms.

467 **Figure 2. Movement-related activity of individual GP neurons**. **A**. Four examples of single
468 neurons, showing average firing rates (top) and spike rasters (bottom) aligned on movement
469 onset (Center Out; correct No-Stop trials only). Activity for contra-, ipsi movements are shown in
470 blue and green respectively. **B**. Top, averaged, Z-scored firing of GP cells around Center Out;
471 time points when activity distinguishes movement direction are shown with thicker lines. Shaded
472 band, +- S.E.M across n=376 neurons. Bottom, fraction of neurons whose firing rate significantly
473 distinguishes movement direction, across time (t-test for each neuron in each 50ms bin,
474 p<0.05). Higher firing rate for contra-, ipsi- shown in blue, green respectively. Horizontal grey

475  lines indicate thresholds for a significant proportion of neurons (binomial test, p<0.05 without or

476  with multiple-comparisons correction respectively) and bins that exceed these thresholds are

477  filled in color. Many GP cells encoded movement direction even before Center-Out; this is less

478  obvious after averaging. **C**. Firing pattern of all GP cells (n=376) on correct contra trials. Activity

479  is scaled between minimum and maximum firing rate across alignments to Go cue (left), Center

480  Out (middle) and the Stop cue (right). In each column cell order (top-bottom) is sorted using the

481  time of peak deflection from average firing, separately for cells that showed bigger increases

482  (top) or decreases (bottom). **D**. GP population activity is more related to movements than cues.

483  Scatter plots show peak deflections in firing rate (Z-scored) for each GP cell, comparing Center

484  Out aligned data to Go cue aligned (top) or Stop cue aligned (bottom). Data included is 500ms

485  around alignment time. Indicated p-values are from Wilcoxon signed rank tests over the GP

486  population; individual GP cells that showed significant differences are indicated with red points (t

487  test, p<0.05). **E**. Scatter plot indicates no overall movement direction bias. Same format, same

488  statistical tests as D, but comparing peak deflections in Center Out aligned firing rate for contra,

489  ipsi movements. **F**. Top, comparing average firing between Maybe-Stop and No-Stop

490  conditions. On left, data is aligned on Go cue, including all Maybe-Stop-Contra trials (including

491  both contra- and ipsi-instructing Go cues and Stop trials). On right, data is aligned on Center-

492  Out (and does not include Stop cue trials). Bottom, proportion of neurons whose firing rate is

493  significantly affected by proactive inhibition (same format as B; bins exceeding p<0.05 threshold

494  without multiple comparisons correction are filled in light color, bins exceeding corrected

495  threshold are filled in dark color. Although GP neurons significantly distinguished Maybe-Stop

496  and No-Stop conditions at multiple time points before the Go cue, there was no single time point

497  at which the proportion of individually-significant neurons became large. **G**. Comparison of

498  individual cell activity in Maybe-Stop and No-Stop conditions, during the 500ms epoch

499  immediately before the Go cue.

500  **Figure 3. GP dynamics for Going and Stopping. A**. PCA was performed using averaged,

501  normalized firing rates for each GP cell, in a 500ms epoch around Center Out for contra and ipsi

502  movements (concatenated). **B**. Variance explained by each of the first 10 PCs. **C**. GP state-

503  space trajectories for contra and ipsi movements (blue, green) within the first 3 PCs, shown from

504  2 different angles. Each small dot along the trajectory is separated by 4ms. Trajectories begin at

505  a similar mean location at the Go cue (diamonds), and diverge gradually until Center Out (large

506  circles) then rapidly thereafter. "Initiation Axis" joins the average position at Go cue and the

507  average position at Center Out (black asterisk). "Selection Axis" joins the means of each

508 trajectory, colored asterisks. **D**. Comparing state-space trajectories for Successful- and Failed-

509 Stop trials. Same format and PCA space as C, but plotting trajectories aligned on the Stop cue

510 (including both contra and ipsi trials). Filled circles indicate epochs of significant Euclidean

511 distance between two trajectories (permutation test on each 4 ms time bin, p<0.05). **E**.

512 Permutation tests of whether the state-space positions for Successful- and Failed-Stop trials are

513 significantly different, at either the Go cue (top) or the Stop cue (bottom). Positions are

514 compared either in the 10-D PC space (Euclidean distance) or along the Initiation or Selection

515 Axes. Grey distributions show surrogate data from 10000 random shuffles of trial types. Dark

516 grey, most extreme 5% of distributions (one-tailed for Euclidean, 2-tailed for others). Red

517 vertical lines show observed results (bright red, significant; dark red, n.s.). **F**. Distance travelled

518 along Initiation Axis for successful and failed Stop trials, aligned on either Go cue (left) or Stop

519 cue (right). Thicker lines indicate epochs of significant difference to the Correct trajectory

520 (permutation test on each 4 ms time bin, p<0.05). On Failed stops (only), activity has already

521 evolved substantially by the time of the Stop cue.

522 **Figure 4. Distinct state-space positions at Go cue predict distinct outcomes**. **A**.

523 Alternative concepts for proactive inhibition, illustrated using a simplified rise-to-threshold

524 framework (Brown & Heathcote2008; Verbruggen & Logan2008; Noorani & Carpenter2016). **B**.

525 Comparison of GP population state between Maybe-Stop-Contra trials (including both contra-

526 and ipsi-instructing Go cues and Stop trials) and No-Stop trials (±100ms around Go cue; same

527 state-space as Fig.3). Filled circles indicate epochs of significant Euclidean distance between

528 two trajectories (permutation test on each 4 ms time bin, p<0.05). **C**. Permutation tests (same

529 format as Fig. 3). Just before the Go cue (-100-0ms) the Maybe-Stop state was significantly

530 shifted away from action initiation, and in the ipsi direction. **D**. Breakdown of GP state for trials

531 with contra Go cues, by distinct trial outcomes. **E**. Quantification of D, comparing evolution of

532 activity along Initiation and Selection Axes on correct contra trials (blue), incorrect action

533 selections (light green) and RT limit errors (brown; failure to initiate movement within 800ms).

534 Thicker lines indicate epochs of significant difference to the Correct trajectory (permutation test

535 on each 4 ms time bin, p<0.05).

536 **Figure 5. Multiple dynamics underlying slower reaction times**. **A**. Comparison of GP

537 population state between correct Maybe-Stop (contra) and No-Stop (contra) trials (-100 to

538 +250ms around Go cue; same state-space and format as Fig.3,4). Time points of significant

539 Euclidean separation between conditions are marked by filled circles. **B**. Permutation tests

19

540   (same format as Fig.3,4) comparing Maybe-Stop (contra) and No-Stop (contra) trials at the time

541   of contra Go cue presentation. GP activity is significantly biased in the ipsi direction, when the

542   contra-instructing cue might be followed by a Stop cue. **C**. Examination of distance travelled

543   after Go cue confirms that in the Maybe-Stop condition the trajectory first moves primarily along

544   the Selection Axis (left), before making substantial progress along the Initiation Axis (right). **D-F**.

545   Same as A-C, but comparing correct contra No-Stop trials with faster or slower RTs (median

546   split of RTs). Unlike Maybe-Stop trials, spontaneously slow RT trials do not show a starting bias

547   (on either Initiation or Selection axes) and do not move on the Selection Axis before moving on

548   the Initiation Axis.

549   **Figure 6. Defining Initiation, Selection Axes with or without prior dimension reduction. A,**

550   Replotting major results from Figs. 3-5 in two dimensions. The Initiation and Selection Axes are

551   defined as in the main figures, i.e. using points in the 10-D PC space. **B,** same as A, but

552   defining axes in the full 376-D state space (skipping the PCA step).

553

554   **Figure 1-figure supplement 1. Behavioral data for all sessions and for each individual**

555   **animal. A**. Proactive slowing of RT is visible in aggregate across all recorded sessions (n= 251

556   sessions, from 6 rats), in both left and right directions. Shading indicates SEM across rats. **B**.

557   Cumulative density plots of RT for all sessions included in electrophysiology data analysis for

558   each rat, in the same format as Fig. 1. Left plots, comparison of Go RT and Stop-fail RT; right

559   plots, selective proactive inhibition for movements contraversive to the recorded neurons.

560

561   **Figure 2-figure supplement 1.  Further details of GP recordings. A**. Estimated locations of

562   recorded units, within coronal atlas sections (Paxinos & Watson 2006). **B**. Firing pattern of all

563   GP cells (n=376) on ipsi trials, shown in the same format as Fig. 2C. **C**. Proactive effects on

564   average GP firing. As Fig. 2F, but dividing units into those that predominantly increase or

565   decrease firing rate. **D**. Duration of significant difference between Maybe-Stop and No-Stop

566   conditions, during the 500ms before Go cue, for each neuron. Most units show a significant

567   difference at some time, but very few show sustained changes with proactive inhibition. **E**.

568   Comparing average GP firing on Correct contra trials and error trials (wrong choices and RT

569   limit errors).

570

**Figure 3-figure supplement 1. Principal Components. A.** The first 10 principal components. **B**. Relative contributions of each PC to the Initiation and Selection Axes (i,e, the eigenvector of each Axis in the 10-PC space). **C**. Weight of each GP neuron on the Initiation and Selection Axis. **D,E**. Spatial arrangement of absolute weight values.

**Figure 4 -figure supplement 1. Neural population results for individual rats, and corresponding behavior. A.** Comparing proactive shifts along Initiation and Selection Axes for all rats together (left) and for individual rats. Rats 2,4 and 6 were grouped together as they had fewer recorded neurons. In left plots, thicker lines indicate epochs of significant difference between two conditions (permutation test on each 4 ms time bin, p<0.05). Note that Rat 3 had the largest Selection Axis bias *towards* ipsiversive movements before the Go cue (and a bias towards movement on the Initiation Axis). **B**. RT results for the same animal groupings. In all cases there was a greater slowing of contra than ipsi movements, consistent with a selective proactive inhibition effect. However, Rat 3 showed a *speeding* of ipsi movements compared to the No-Stop condition, consistent with an ipsiversive bias and no overall movement inhibition.

**Figure 4 -figure supplement 2. Trial-history dependence. A.** (Left) On Maybe-Stop trials that followed Stop trials ("After-Stop"), rats were more likely to succeed in stopping (Wilcoxon signed rank test, z=2.67, p=0.008) and showed increased RT (Wilcoxon signed rank test, z=4.46, p=8.02×10$^{-6}$), compared to trials that followed Go trials. (Right) On No-Stop trials that followed error trials ("After-Error"), rats were more likely to make RT limit errors (Wilcoxon signed rank test, z=3.03, p=0.002) and showed increased RT (Wilcoxon signed rank test, z=5.42, p=5.95×10$^{-8}$). **B.** Corresponding apparent shifts along the Initiation Axis did not reach significance (permutation tests, analysis epoch: -100 - 0ms before Go cue).

**Figure 5 -figure supplement 1. Comparison of RT-matched Maybe-Stop and No-Stop trajectories. A-C**, same as Fig. 5 A-C but using RT-matched subsets of trials. For RT matching, each RT from the Maybe-Stop condition was paired with the closest RT from the No-Stop condition; if no pair could be found within 250ms, the trial was not used. After RT matching the mean Maybe-Stop RT was 371ms (median 370ms) and the median No-Stop RT was 369ms (median 360ms). **D-F**, same as A-C but aligned on movement onset (Center out).

**Figure 5 -figure supplement 2. Comparison of Proactive and spontaneously Slow RT trajectories at movement onset.** All panels are as Fig. 5, but aligned on movement onset (Center out).

21

602

**Video 1. Using movement-related trajectories through state-space to define Initiation, Selection Axes.**

**Video 2. State-space location at the Go cue varies with distinct types of errors.**

**Video 3. Comparing neural trajectories for correct, contra Maybe-Stop versus No-Stop trials.**

608

## References

Ames, K Cora, Stephen I Ryu, and Krishna V Shenoy. "Simultaneous Motor Preparation and Execution in a Last-moment Reach Correction Task." *Nature communications* 10, no. 1 (2019): doi:10.1038/s41467-019-10772-2.

Abecassis, ZA, Berceau BL, Win PH. *et al.* "Npas1+-Nkx2.1+Neurons Are An Integral Part of the Cortico-pallido-cortical Loop." *Journal of neuroscience* 40, no. 4 (2020): doi:10.1523/JNEUROSCI.1199-19.2019.

Afshar A, Santhanam G, Yu BM, Ryu SI, Sahani M, Shenoy KV. Single-trial neural correlates of arm movement preparation. *Neuron.* 2011 Aug 11;71(3):555-64.

Arkadir, David, Genela Morris, Eilon Vaadia, and Hagai Bergman. "Independent Coding of Movement Direction and Reward Prediction by Single Pallidal Neurons." *Journal of neuroscience* 24, no. 45 (2004): doi:10.1523/JNEUROSCI.2583-04.2004.

Aron, Adam R, and Russell A Poldrack. "Cortical and Subcortical Contributions to Stop Signal Response Inhibition: Role of the Subthalamic Nucleus." *Journal of neuroscience* 26, no. 9 (2006): doi:10.1523/JNEUROSCI.4682-05.2006.

Aron, Adam R, and Frederick Verbruggen. "Stop the Presses: Dissociating a Selective From a Global Mechanism for Stopping." *Psychol Sci* 19, no. 11 (2008): doi:10.1111/j.1467-9280.2008.02216.x.

Aron AR. From reactive to proactive and selective control: developing a richer model for stopping inappropriate responses. *Biol Psychiatry.* 2011 Jun 15;69(12):e55-68.

Aron, Adam R, Trevor W Robbins, and Russell A Poldrack. "Inhibition and the Right Inferior Frontal Cortex: One Decade On." *Trends in cognitive sciences* 18, no. 4 (2014): doi:10.1016/j.tics.2013.12.003.

Brotchie, P, R Iansek, and M K Horne. "Motor Function of the Monkey Globus Pallidus. 2. Cognitive Aspects of Movement and Phasic Neuronal Activity." *Brain : a journal of neurology* 114 ( Pt 4) (1991): doi:10.1093/brain/114.4.1685.

Brown, Scott D, and Andrew Heathcote. "The Simplest Complete Model of Choice Response Time: Linear Ballistic Accumulation." *Cogn Psychol* 57, no. 3 (2008): doi:10.1016/j.cogpsych.2007.12.002.

Cai W, Oldenkamp CL, Aron AR. A proactive mechanism for selective suppression of response tendencies. *J Neurosci.* 2011 Apr 20;31(16):5965-9.

Carli, M, J L Evenden, and T W Robbins. "Depletion of Unilateral Striatal Dopamine Impairs Initiation of Contralateral Actions and Not Sensory Attention." *Nature* 313, no. 6004 (1985): 679-82.

Cavanagh J, Thomas V Wiecki, Michael X Cohen, Christina M Figueroa, Johan Samanta, Scott J Sherman & Michael J Frank   Subthalamic nucleus stimulation reverses mediofrontal influence over decision threshold. *Nature Neuroscience* volume 14, pages1462–1467(2011)

Chatham, Christopher H, Eric D Claus, Albert Kim, Tim Curran, Marie T Banich, and Yuko Munakata. "Cognitive Control Reflects Context Monitoring, Not Motoric Stopping, in Response Inhibition." *PloS one* 7, no. 2 (2012): e31546-e31546.

Chen CH, KW Scangos, V Stuphorn (2010). Supplementary motor area exerts proactive and reactive control of arm movements. *Journal of Neuroscience* 30 (44), 14657-14675

Chevalier, G, and J M Deniau. "Disinhibition As a Basic Process in the Expression of Striatal Functions." *Trends in neurosciences* 13, no. 7 (1990): 277-80.

Chikazoe, Junichi, Koji Jimura, Tomoki Asari, Ken-ichiro Yamashita, Hiroki Morimoto, Satoshi Hirose, Yasushi Miyashita, and Seiki Konishi. "Functional Dissociation in Right Inferior Frontal Cortex During Performance of Go/no-go Task." *Cerebral cortex* (New York, N.Y. : 1991) 19, no. 1 (2009): doi:10.1093/cercor/bhn065.

Chung JE, Magland JF, Barnett AH, Tolosa VM, Tooker AC, Lee KY, Shah KG, Felix SH, Frank LM, Greengard LF. A fully automated approach to spike sorting. *Neuron.* 2017 Sep 13;95(6):1381-1394

Collins, Anne G E, and Michael J Frank. "Opponent Actor Learning (OpAL): Modeling Interactive Effects of Striatal Dopamine on Reinforcement Learning and Choice Incentive." *Psychological review* 121, no. 3 (2014): doi:10.1037/a0037015.

Cunningham JP, Yu BM. Dimensionality reduction for large-scale neural recordings. Nature Neuroscience 17, p.1500–1509 (2014)

DeLong, M R. "Activity of Pallidal Neurons During Movement." Journal of neurophysiology 34, no. 3 (1971): 414-427.

Dunovan, Kyle, Brighid Lynch, Tara Molesworth, and Timothy Verstynen. "Competing Basal Ganglia Pathways Determine the Difference Between Stopping and Deciding Not to Go." eLife 4 (2015): e08723.

Eagle DM, Baunez C, Hutcheson DM, Lehmann O, Shah AP, Robbins TW. Stop-signal reaction-time task performance: role of prefrontal cortex and subthalamic nucleus. Cereb Cortex. 2008 Jan;18(1):178-88.

Elsayed GF, Lara AH, Kaufman MT, Churchland MM, Cunningham JP. Reorganization between preparatory and movement population responses in motor cortex. Nat Commun. 2016 Oct 27;7:13239.

Ersche, Karen D, P Simon Jones, Guy B Williams, Abigail J Turton, Trevor W Robbins, and Edward T Bullmore. "Abnormal Brain Structure Implicated in Stimulant Drug Addiction." Science (New York, N.Y.) 335, no. 6068 (2012): doi:10.1126/science.1214463.

GJ Gage, CR Stoetzner, AB Wiltschko, JD Berke. Selective activation of striatal fast-spiking interneurons during choice execution. (2010) Neuron 67 (3), 466-479

Gardiner, T W, and S T Kitai. "Single-unit Activity in the Globus Pallidus and Neostriatum of the Rat During Performance of a Trained Head Movement." Experimental brain research 88, no. 3 (1992): 517-30.

Gurney, TJ Prescott, P Redgrave. A computational model of action selection in the basal ganglia. I. A new functional anatomy. (2001) Biological cybernetics 84 (6), 401-410

Haith AM, J Pakpoor, JW Krakauer. Independence of movement preparation and movement initiation Journal of Neuroscience 36 (10), 3007-3015

Hanes, D P, and J D Schall. "Neural Control of Voluntary Movement Initiation." Science (New York, N.Y.) 274, no. 5286 (1996): 427-30.

Hardung S, Epple R, Jäckel Z, Eriksson D, Uran C, Senn V, Gibor L, Yizhar O, Diester I. A Functional Gradient in the Rodent Prefrontal Cortex Supports Behavioral Inhibition. Curr Biol. 2017 Feb 20;27(4):549-555.

Isoda, Masaki, and Okihide Hikosaka. "Role for Subthalamic Nucleus Neurons in Switching From Automatic to Controlled Eye Movement." The Journal of neuroscience : the official journal of the Society for Neuroscience 28, no. 28 (2008): doi:10.1523/JNEUROSCI.0487-08.2008.

Jahanshahi M, Obeso I, Rothwell JC, Obeso JA. A fronto-striato-subthalamic-pallidal network for goal-directed and habitual inhibition. Nat Rev Neurosci. 2015 Dec;16(12):719-32.

Jahfari, S, F Verbruggen, M J Frank, L J Waldorp, L Colzato, K R Ridderinkhof, and B U Forstmann. "How Preparation Changes the Need for Top-Down Control of the Basal Ganglia When Inhibiting Premature Actions." Journal of neuroscience 32, no. 32 (2012),

Kim HF, Amita H, Hikosaka O. Indirect Pathway of Caudal Basal Ganglia for Rejection of Valueless Visual Objects. Neuron. 2017 May 17;94(4):920-930.

Kaufman MT, Churchland MM, Ryu SI, Shenoy KV. Cortical activity in the null space: permitting preparation without movement. Nat Neurosci. 2014 Mar;17(3):440-8.

Kaufman, M. T. et al. The Largest Response Component in the Motor Cortex Reflects Movement Timing but Not Movement Type. Eneuro 3, ENEURO.0085-16.2016 (2016).

Kawagoe, R, Y Takikawa, and O Hikosaka. "Expectation of Reward Modulates Cognitive Signals in the Basal Ganglia." *Nature neuroscience* 1, no. 5 (1998): 411-6.

Kim, Hyoung F, Hidetoshi Amita, and Okihide Hikosaka. "Indirect Pathway of Caudal Basal Ganglia for Rejection of Valueless Visual Objects." Neuron 94, no. 4 (2017): doi:10.1016/j.neuron.2017.04.033.

Klaus, Andreas, Joaquim Alves da Silva, and Rui M Costa. "What, If, and When to Move: Basal Ganglia Circuits and Self-Paced Action Initiation." Annual review of neuroscience 42 (2019): doi:10.1146/annurev-neuro-072116-031033.

Kravitz, BS Freeze, PRL Parker, K Kay, MT Thwin, K Deisseroth, ...Regulation of parkinsonian motor behaviours by optogenetic control of basal ganglia circuitry. Nature 466 (7306), 622-626

Leunissen I, Coxon JP, Swinnen SP. A proactive task set influences how response inhibition is implemented in the basal ganglia. Hum Brain Mapp. 2016 Dec;37(12):4706-4717.

Leventhal, Daniel K, Gregory J Gage, Robert Schmidt, Jeffrey R Pettibone, Alaina C Case, and Joshua D Berke. "Basal Ganglia Beta Oscillations Accompany Cue Utilization." *Neuron* 73, no. 3 (2012): doi:10.1016/j.neuron.2011.11.032.

Leventhal, Daniel K, Colin Stoetzner, Rohit Abraham, Jeff Pettibone, Kayla DeMarco, and Joshua D Berke. "Dissociable Effects of Dopamine on Learning and Performance Within Sensorimotor Striatum." *Basal ganglia* 4, no. 2 (2014): doi:10.1016/j.baga.2013.11.001.

Lipszyc, Jonathan, and Russell Schachar. "Inhibitory Control and Psychopathology: A Meta-analysis of Studies Using the Stop Signal Task." *J Int Neuropsychol Soc* 16, no. 6 (2010): doi:10.1017/S1355617710000895.

Logan, G D, W B Cowan, and K A Davis. "On the Ability to Inhibit Simple and Choice Reaction Time Responses: A Model and a Method." *J Exp Psychol Hum Percept Perform* 10, no. 2 (1984): 276-91.

Majid DS, Cai W, Corey-Bloom J, Aron AR. Proactive selective response suppression is implemented via the basal ganglia. J Neurosci. 2013 Aug 14;33(33):13259-69

735   Mallet N, Schmidt R, Leventhal D, Chen F, Amer N, Boraud T, Berke JD. Arkypallidal Cells
736       Send a Stop Signal to Striatum. Neuron. 2016 Jan 20;89(2):308-16.

737   Manohar, Sanjay G, Trevor T-J Chong, Matthew A J Apps, Amit Batla, Maria Stamelou, Paul R
738       Jarman, Kailash P Bhatia, and Masud Husain. "Reward Pays the Cost of Noise Reduction in
739       Motor and Cognitive Control." Current biology : CB 25, no. 13 (2015):
740       doi:10.1016/j.cub.2015.05.038.

741   Mayse JD, Nelson GM, Park P, Gallagher M, Lin SC. Proactive and reactive inhibitory control in
742       rats. Front Neurosci. 2014 May 8;8:104.

743   Meyer, Heidi C, and David J Bucci. "Neural and Behavioral Mechanisms of Proactive and
744       Reactive Inhibition." *Learning & memory (Cold Spring Harbor, N.Y.)* 23, no. 10 (2016):
745       doi:10.1101/lm.040501.115.

746   Noorani, Imran, and R H S Carpenter. "The LATER Model of Reaction Time and Decision."
747       *Neuroscience and biobehavioral reviews* 64 (2016): doi:10.1016/j.neubiorev.2016.02.018.

748   Paxinos, C Watson - The rat brain in stereotaxic coordinates. 2006

749   Roseberry, Thomas K, A Moses Lee, Arnaud L Lalive, Linda Wilbrecht, Antonello Bonci, and
750       Anatol C Kreitzer. "Cell-Type-Specific Control of Brainstem Locomotor Circuits by Basal
751       Ganglia." Cell 164, no. 3 (2016): doi:10.1016/j.cell.2015.12.037.

752   Pouget, Pierre, Gordon D Logan, Thomas J Palmeri, Leanne Boucher, Martin Paré, and Jeffrey
753       D Schall. "Neural Basis of Adaptive Response Time Adjustment During Saccade
754       Countermanding." *The Journal of neuroscience : the official journal of the Society for
755       Neuroscience* 31, no. 35 (2011): doi:10.1523/JNEUROSCI.1868-11.2011.

756   Schmidt R, Leventhal DK, Mallet N, Chen F, Berke JD. Canceling actions involves a race
757       between basal ganglia pathways. Nat Neurosci. 2013 Aug;16(8):1118-24.

758   Schmidt, Robert, and Joshua D Berke. "A Pause-then-Cancel Model of Stopping: Evidence
759       From Basal Ganglia Neurophysiology." *Philosophical transactions of the Royal Society of
760       London. Series B, Biological sciences* 372, no. 1718 (2017)doi:10.1098/rstb.2016.0202.

761   Shin S, Sommer MA. Activity of neurons in monkey globus pallidus during oculomotor behavior
762       compared with that in substantia nigra pars reticulata. J Neurophysiol. 2010
763       Apr;103(4):1874-87

764   Smith, P L, and R Ratcliff. "Psychology and Neurobiology of Simple Decisions." *Trends in
765       neurosciences* 27, no. 3 (2004): 161-8.

766   Stanford, Terrence R, Swetha Shankar, Dino P Massoglia, M Gabriela Costello, and Emilio
767       Salinas. "Perceptual Decision Making in Less Than 30 Milliseconds." Nature neuroscience
768       13, no. 3 (2010): doi:10.1038/nn.2485.

769   Swann N, Nitin Tandon, Ryan Canolty, Timothy M. Ellmore, Linda K. McEvoy, Stephen Dreyer,
770       Michael DiSano and Adam R. Aron. Intracranial EEG Reveals a Time- and Frequency-
771       Specific Role for the Right Inferior Frontal Gyrus and Primary Motor Cortex in Stopping
772       Initiated Responses. Journal of Neuroscience 7 October 2009, 29 (40) 12675-12685

773   Thura D, Cisek P. The basal ganglia do not select reach targets but control the urgency of
774       commitment. Neuron. 2017 Aug 30;95(5):1160-1170

775   Turner, R S, and M E Anderson. "Pallidal Discharge Related to the Kinematics of Reaching
776       Movements in Two Dimensions." Journal of neurophysiology 77, no. 3 (1997): 1051-74

777 Verbruggen, Frederick, and Gordon D Logan. "Proactive Adjustments of Response Strategies in
778     the Stop-signal Paradigm." *Journal of experimental psychology. Human perception and*
779     *performance* 35, no. 3 (2009): doi:10.1037/a0012726.

780 Verbruggen, Frederick, Adam R Aron, Guido Ph Band, Christian Beste, Patrick G Bissett, Adam
781     T Brockett, Joshua W Brown, and others. "A Consensus Guide to Capturing the Ability to
782     Inhibit Actions and Impulsive Behaviors in the Stop-signal Task." eLife 8 (2019)
783     doi:10.7554/eLife.46323.

784 Wessel, Jan R, and Adam R Aron. "On the Globality of Motor Suppression: Unexpected Events
785     and Their Influence on Behavior and Cognition." Neuron 93, no. 2 (2017):
786     doi:10.1016/j.neuron.2016.12.013.

787 Wiltschko, A B, G J Gage, and J D Berke. "Wavelet Filtering Before Spike Detection Preserves
788     Waveform Shape and Enhances Single-unit Discrimination." *J Neurosci Methods* 173, no. 1
789     (2008): 34-40.

790 Yoshida, Atsushi, and Masaki Tanaka. "Two Types of Neurons in the Primate Globus Pallidus
791     External Segment Play Distinct Roles in Antisaccade Generation." Cerebral cortex (New
792     York, N.Y. : 1991) 26, no. 3 (2016): doi:10.1093/cercor/bhu308.

793 Yoshida J, Saiki A, Soma S, Yamanaka K, Nonomura S, Ríos A, Kawabata M, Kimura M, Sakai
794     Y, Isomura Y. Area-specific Modulation of Functional Cortical Activity During Block-based
795     and Trial-based Proactive Inhibition. Neuroscience. 2018 Sep 15;388:297-316.

796 Zandbelt, Bram B, Mirjam Bloemendaal, Sebastiaan F W Neggers, René S Kahn, and Matthijs
797     Vink. "Expectations and Violations: Delineating the Neural Network of Proactive Inhibitory
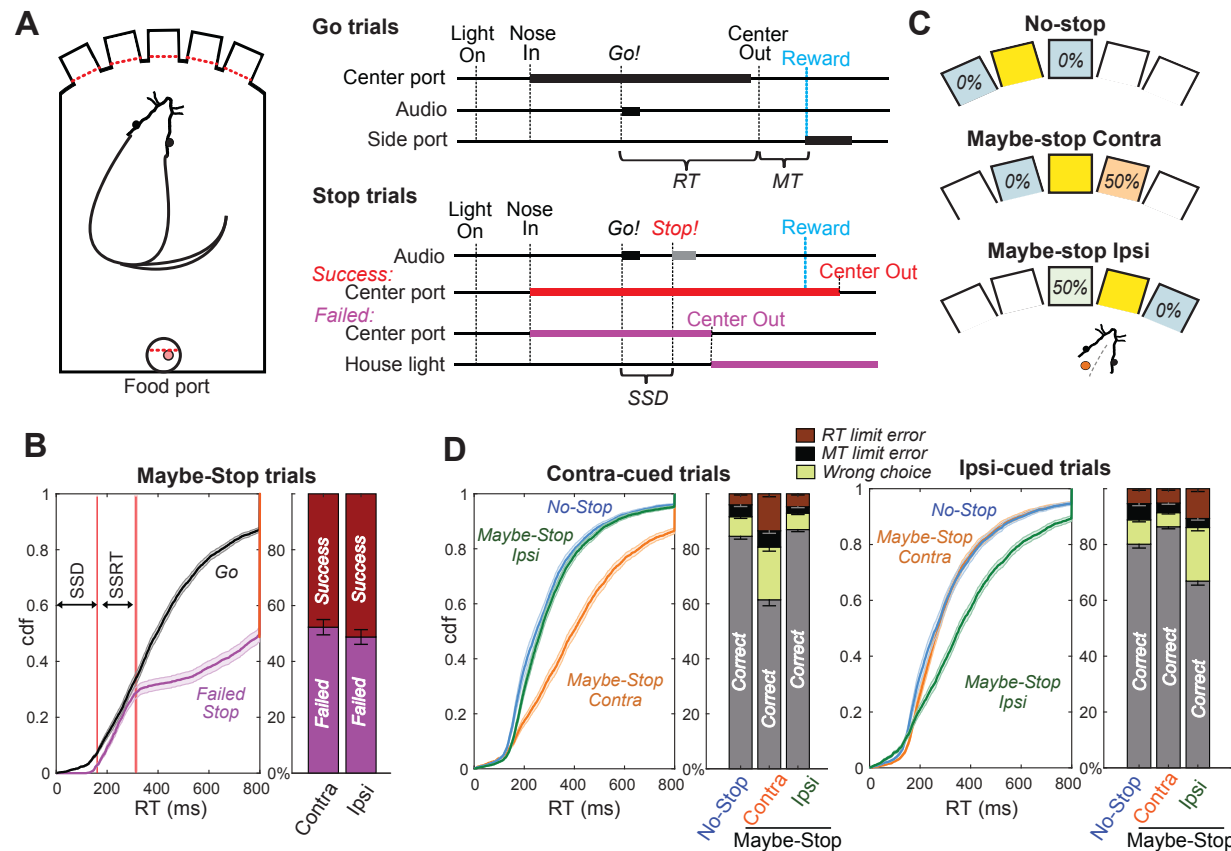798     Control." Hum Brain Mapp (2012) doi:10.1002/hbm.22047.

**Figure 1. Reactive and Proactive Behavioral Inhibition**.

**A**. Left, operant box configuration; right, event sequence for Go and Stop trials. RT, reaction time; MT, movement time; SSD, stop-signal delay; Reward, delivery of a sugar pellet to the food port.

**B**. Left, distributions of Go and Failed-Stop RTs (on Maybe-Stop trials; shading, S.E.M. across n = 63 sessions). Failed-Stop RTs are similar to the faster part of the Go RT distribution, consistent with the "race" model in which a relatively-fast Go process produces failures to stop. The tail of the Failed-Stop distribution (RT > 500ms) is presumed to reflect trials for which rats successfully responded to the Stop cue, but then failed to maintain holding until reward delivery (see Leventhal et al. 2012; Schmidt et al. 2013; Mayse et al. 2014). Right, proportions of failed and successful Stop trials after Contra and Ipsi Go cues. Error bars, S.E.M. across n=63 sessions.

**C**. Trial start location indicates stop probabilities (locations counterbalanced across rats). In this example configuration recording from left GP, starting from the middle hole indicates the Maybe-stop Contra condition: Go cues instructing rightward movements might be followed by a Stop cue, but Go cues instructing leftward movements will not.

**D**. Proactive inhibition causes selective RT slowing for the Maybe-Stop direction (two-tail Wilcoxon signed rank tests on median RT for each session: contra cues in Maybe-Stop-contra versus No-Stop, z=7.7, p=1.15×10$^{-14}$; ipsi cues in Maybe-Stop-contra versus No-Stop, p=0.32). Additionally, under selective proactive inhibition rats were more likely to fail to respond quickly enough (RT limit errors; Wilcoxon signed rank tests, z=7.2, p=5.41×10$^{-13}$) and to select the wrong choice (uncued action direction; Wilcoxon signed rank tests, z=7.0, p=2.59×10$^{-12}$). Error bars, S.E.M. across n=63 sessions. Only trials without a Stop cue are included here. *RT limit error* = Nose remained in Center port for >800ms after Go cue onset; *MT limit error* = movement time between Center Out and Side port entry > 500ms.
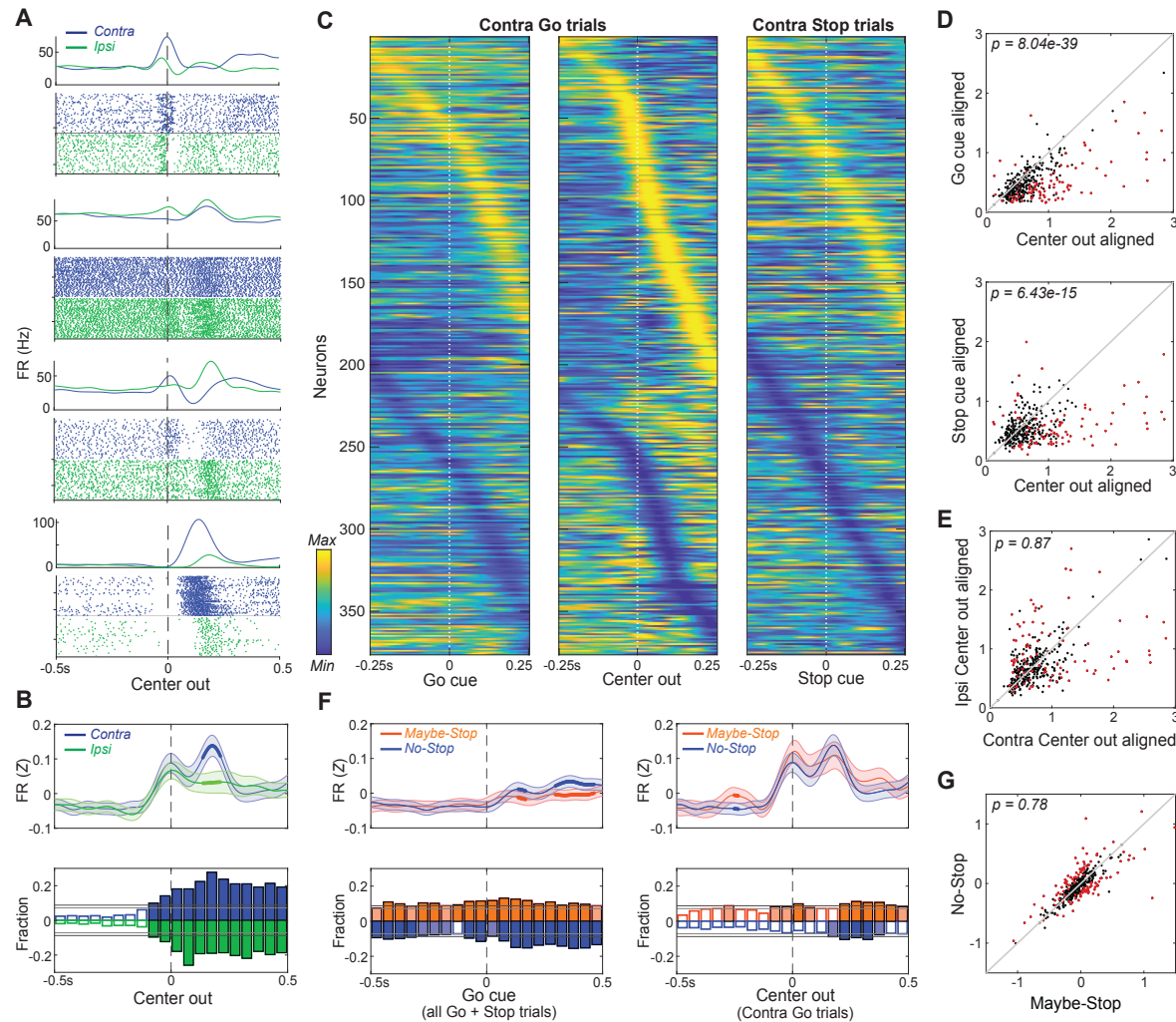
## Figure 2



**Figure 2. Movement-related activity of individual GP neurons.**

**A**. Four examples of single neurons, showing average firing rates (top) and spike rasters (bottom) aligned on movement onset (Center Out; correct No-Stop trials only). Activity for contra-, ipsi movements are shown in blue and green respectively.

**B**. Top, averaged, Z-scored firing of GP cells around Center Out; time points when activity distinguishes movement direction are shown with thicker lines. Shaded band, +- S.E.M across n=376 neurons. Bottom, fraction of neurons whose firing rate significantly distinguishes movement direction, across time (t-test for each neuron in each 50ms bin, p<0.05). Higher firing rate for contra-, ipsi- shown in blue, green respectively. Horizontal grey lines indicate thresholds for a significant proportion of neurons (binomial test, p<0.05 without or with multiple-comparisons correction respectively) and bins that exceed these thresholds are filled in color. Many GP cells encoded movement direction even before Center-Out; this is less obvious after averaging.

**C**. Firing pattern of all GP cells (n=376) on correct contra trials. Activity is scaled between minimum and maximum firing rate across alignments to Go cue (left), Center Out (middle) and the Stop cue (right). In each column cell order (top-bottom) is sorted using the time of peak deflection from average firing, separately for cells that showed bigger increases (top) or decreases (bottom).

**D**. GP population activity is more related to movements than cues. Scatter plots show peak deflections in firing rate (Z-scored) for each GP cell, comparing Center Out aligned data to Go cue aligned (top) or Stop cue aligned (bottom). Data included is 500ms around alignment time. Indicated p-values are from Wilcoxon signed rank tests over the GP population; individual GP cells that showed significant differences are indicated with red points (t test, p<0.05).

**E**. Scatter plot indicates no overall movement direction bias. Same format, same statistical tests as D, but comparing peak deflections in Center Out aligned firing rate for contra, ipsi movements.

**F**. Top, comparing average firing between Maybe-Stop and No-Stop conditions. On left, data is aligned on Go cue, including all Maybe-Stop-Contra trials (including both contra- and ipsi-instructing Go cues and Stop trials). On right, data is aligned on Center-Out (and does not include Stop cue trials). Bottom, proportion of neurons whose firing rate is significantly affected by proactive inhibition (same format as B; bins exceeding p<0.05 threshold without multiple comparisons correction are filled in light color, bins exceeding corrected threshold are filled in dark color. Although GP neurons significantly distinguished Maybe-Stop and No-Stop conditions at multiple time points before the Go cue, there was no single time point at which the proportion of individually-significant neurons became large.

**G**. Comparison of individual cell activity in Maybe-Stop and No-Stop conditions, during the 500ms epoch immediately before the Go cue.

# Figure 3



## Figure 3. GP dynamics for Going and Stopping.

**A**. PCA was performed using averaged, normalized firing rates for each GP cell, in a 500ms epoch around Center Out for contra and ipsi movements (concatenated).

**B**. Variance explained by each of the first 10 PCs.

**C**. GP state-space trajectories for contra and ipsi movements (blue, green) within the first 3 PCs, shown from 2 different angles. Each small dot along the trajectory is separated by 4ms. Trajectories begin at a similar mean location at the Go cue (diamonds), and diverge gradually until Center Out (large circles) then rapidly thereafter. "Initiation Axis" joins the average position at Go cue and the average position at Center Out (black asterisk). "Selection Axis" joins the means of each trajectory, colored asterisks.

**D**. Comparing state-space trajectories for Successful- and Failed-Stop trials. Same format and PCA space as C, but plotting trajectories aligned on the Stop cue (including both contra and ipsi trials). Filled circles indicate epochs of significant Euclidean distance between two trajectories (permutation test on each 4 ms time bin, p<0.05).

**E**. Permutation tests of whether the state-space positions for Successful- and Failed-Stop trials are significantly different, at either the Go cue (top) or the Stop cue (bottom). Positions are compared either in the 10-D PCA space (Euclidean distance) or along the Initiation or Selection Axes. Grey distributions show surrogate data from 10000 random shuffles of trial types. Dark grey, most extreme 5% of distributions (one-tailed for Euclidean, 2-tailed for others). Red vertical lines show observed results (bright red, significant; dark red, n.s.).

**F**. Distance travelled along Initiation Axis for successful and failed Stop trials, aligned on either Go cue (left) or Stop cue (right). Thicker lines indicate epochs of significant difference to the Correct trajectory (permutation test on each 4 ms time bin, p<0.05). On Failed stops (only), activity has already evolved substantially by the time of the Stop cue.

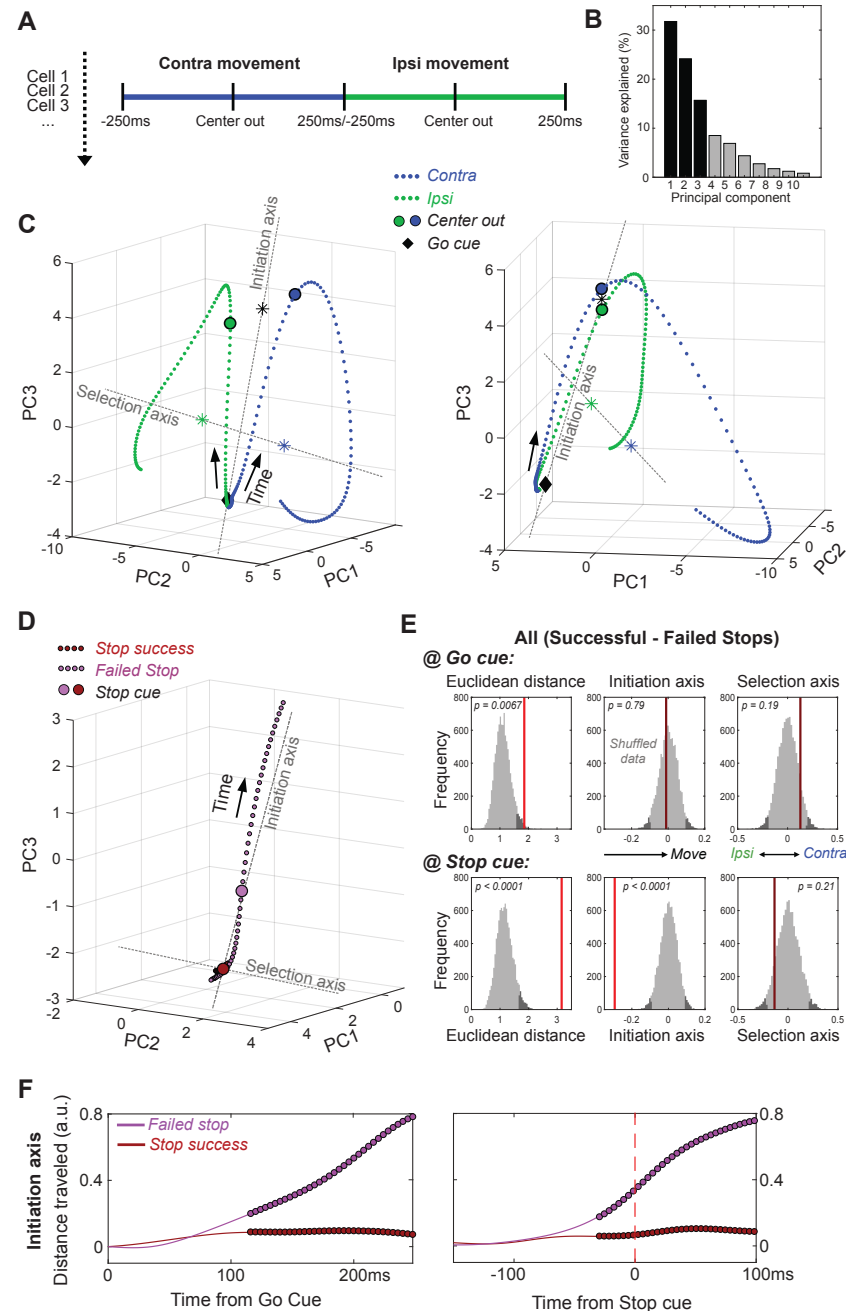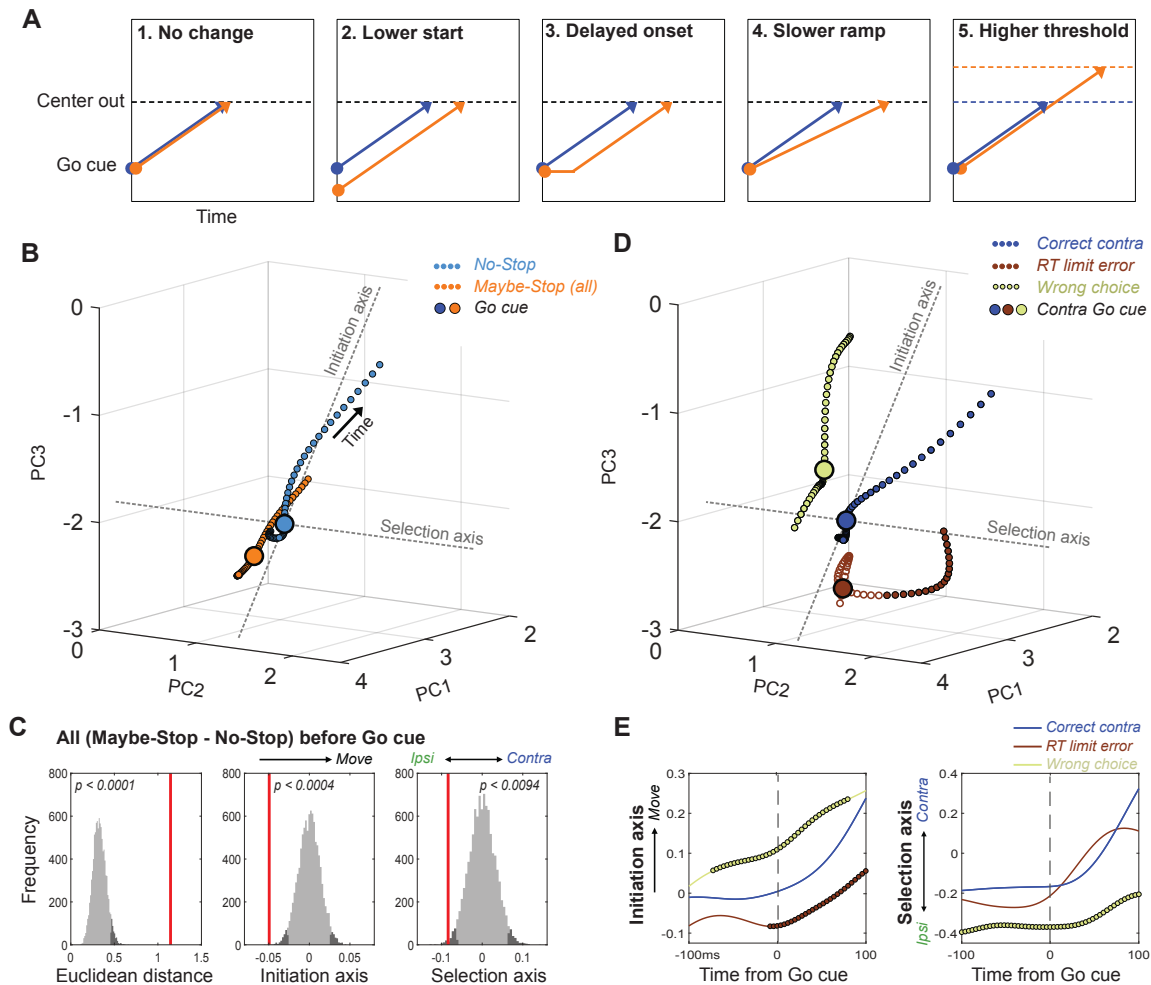# *Figure 4*



**Figure 4. Distinct state-space positions at Go cue predict distinct outcomes**.

**A**. Alternative concepts for proactive inhibition, illustrated using a simplified rise-to-threshold framework (Brown & Heathcote 2008; Verbruggen & Logan 2009; Noorani & Carpenter 2016).

**B**. Comparison of GP population state between Maybe-Stop-Contra trials (including both contra- and ipsi-instructing Go cues and Stop trials) and No-Stop trials (±100ms around Go cue; same state-space as Fig.3). Filled circles indicate epochs of significant Euclidean distance between two trajectories (permutation test on each 4 ms time bin, p<0.05).

**C**. Permutation tests (same format as Fig. 3). Just before the Go cue (-100-0ms) the Maybe-Stop state was significantly shifted away from action initiation, and in the ipsi direction.

**D**. Breakdown of GP state for trials with contra Go cues, by distinct trial outcomes. For Wrong Choice and RT limit errors, filled circles indicate epochs of significant Euclidean distance to the corresponding Correct contra time points (permutation test on each 4 ms time bin, p<0.05).

**E**. Quantification of D, comparing evolution of activity along Initiation and Selection Axes on correct contra trials (blue), incorrect action selections (light green) and RT limit errors (brown; failure to initiate movement within 800ms). Thicker lines indicate epochs of significant difference to the Correct trajectory (permutation test on each 4 ms time bin, p<0.05).
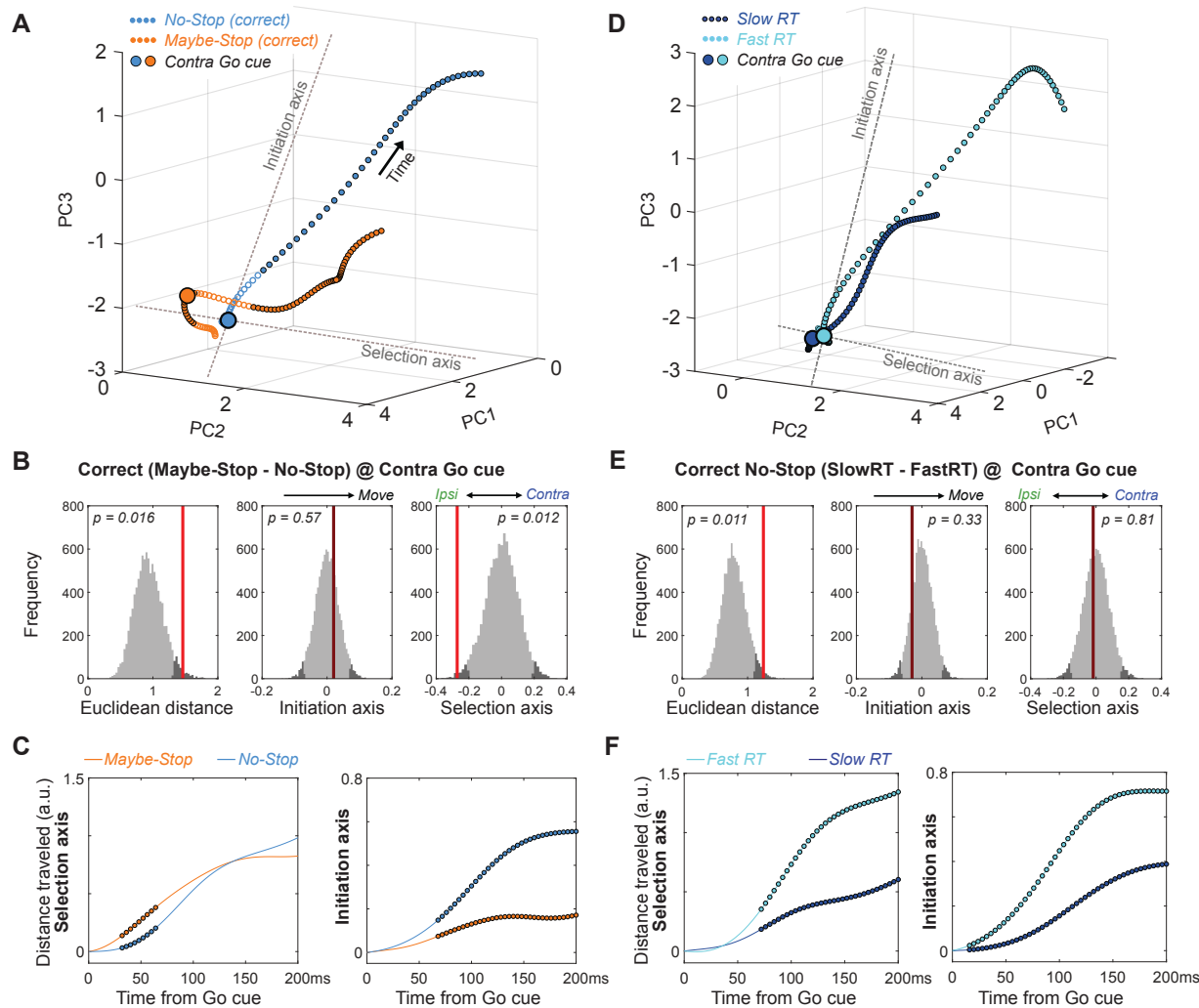
# Figure 5



**Figure 5. Multiple dynamics underlying slower reaction times**.

**A**. Comparison of GP population state between correct Maybe-Stop (contra; only trials without a Stop cue) and No-Stop (contra) trials (-100 to +250ms around Go cue; same state-space and format as Fig.3,4). Time points of significant Euclidean separation between conditions are marked by filled circles.

**B**. Permutation tests (same format as Fig.3,4) comparing Maybe-Stop (contra) and No-Stop (contra) trials at the time of contra Go cue presentation. GP activity is significantly biased in the ipsi direction, when the contra-instructing cue might be followed by a Stop cue.

**C**. Examination of distance travelled after Go cue confirms that in the Maybe-Stop condition the trajectory first moves primarily along the Selection Axis (left), before making substantial progress along the Initiation Axis (right).

**D-F**. Same as A-C, but comparing correct contra No-Stop trials with faster or slower RTs (median split of RTs). Unlike Maybe-Stop trials, spontaneously slow RT trials do not show a starting bias (on either Initiation or Selection axes) and do not move on the Selection Axis before moving on the Initiation Axis.
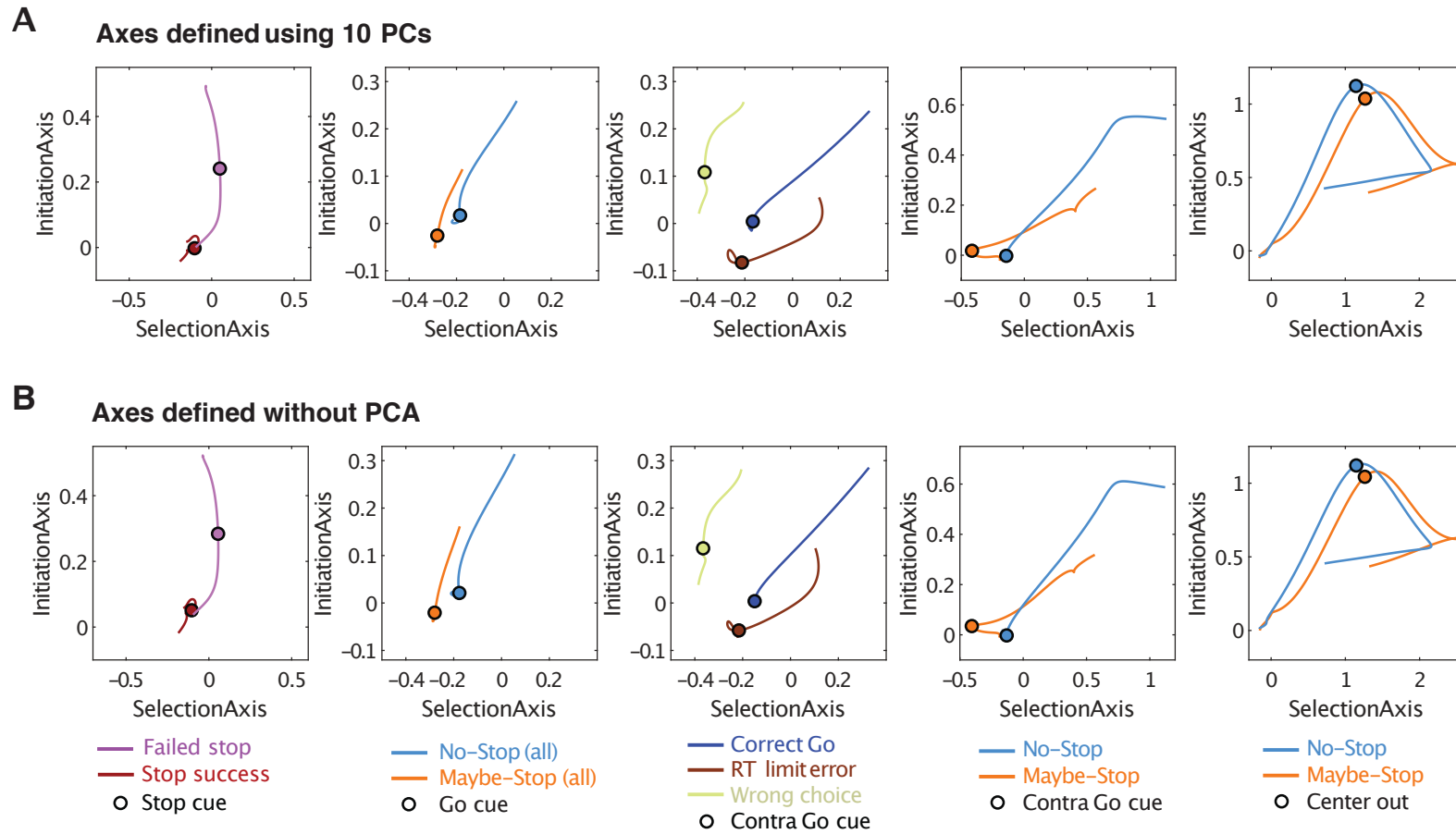
# Figure 6

## A

**Axes defined using 10 PCs**



## B

**Axes defined without PCA**



Legend:
- Failed stop
- Stop success
- Stop cue
- No–Stop (all)
- Maybe–Stop (all)
- Go cue
- Correct Go
- RT limit error
- Wrong choice
- Contra Go cue
- No–Stop
- Maybe–Stop
- Contra Go cue
- No–Stop
- Maybe–Stop
- Center out

**Figure 6. Defining Initiation, Selection Axes with or without prior dimension reduction.**

**A,** Replotting major results from Figs. 3-5 in two dimensions. The Initiation and Selection Axes are defined as in the main figures, i.e. using points in the 10-D PC space.

**B,** same as A, but defining axes in the full 376-D state space (skipping the PCA step).

# Figure 1 - figure supplement 1

**Behavioral data for all sessions and for each individual animal.**

**A**. Proactive slowing of RT is visible in aggregate across all recorded sessions (n= 251 sessions, from 6 rats), in both left and right directions. Shading indicates SEM across rats.

**B**. Cumulative density plots of RT for all sessions included in electrophysiology data analysis for each rat, in the same format as Fig. 1. Left plots, comparison of Go RT and Stop-fail RT; right plots, selective proactive inhibition for movements contraversive to the recorded neurons.
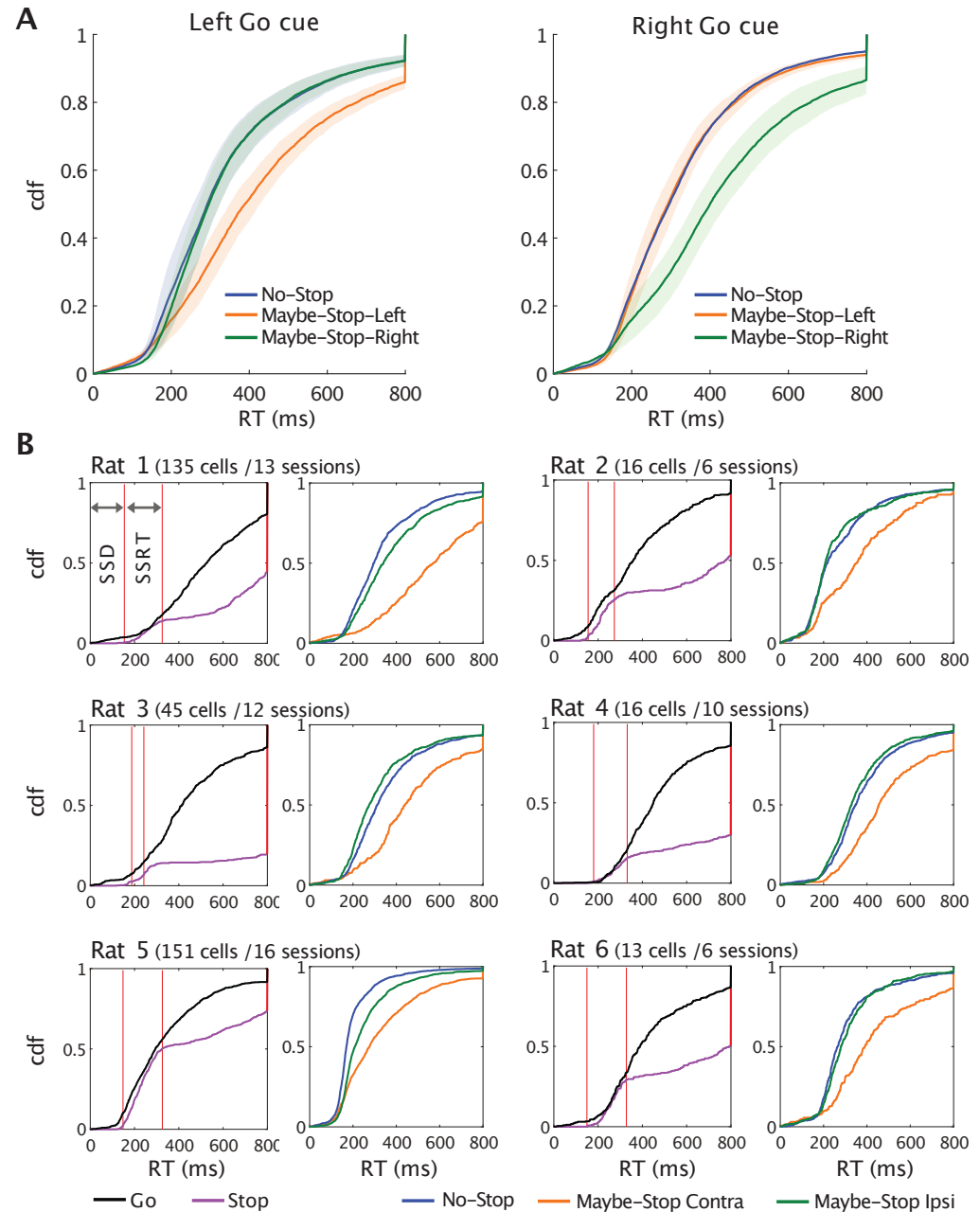
# Figure 2 - figure supplement 1

**Further details of GP recordings.**

**A**. Estimated locations of recorded units, within coronal atlas sections (Paxinos & Watson 2006).

**B.** Firing pattern of all GP cells (n=376) on ipsi trials, shown in the same format as Fig. 2C.

**C**. Proactive effects on average GP firing. As Fig. 2F, but dividing units into those that predominantly increase or decrease firing rate.

**D**. Duration of significant difference between Maybe-Stop and No-Stop conditions, during the 500ms before Go cue), for each neuron. Most units show a significant difference at some time, but very few show sustained changes with proactive inhibition.

**E**. Comparing average GP firing on Correct contra trials and error trials (wrong choices and RT limit errors).
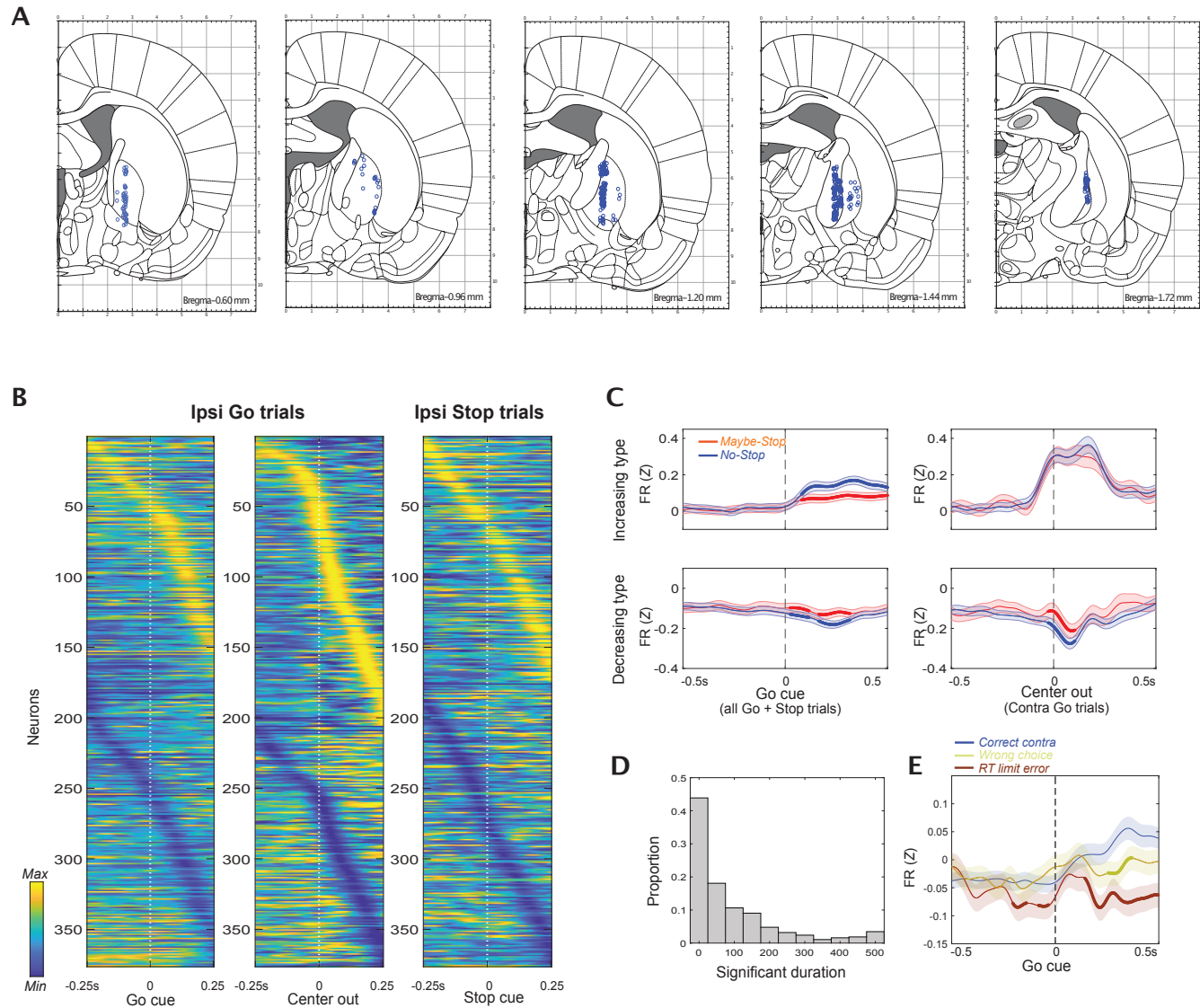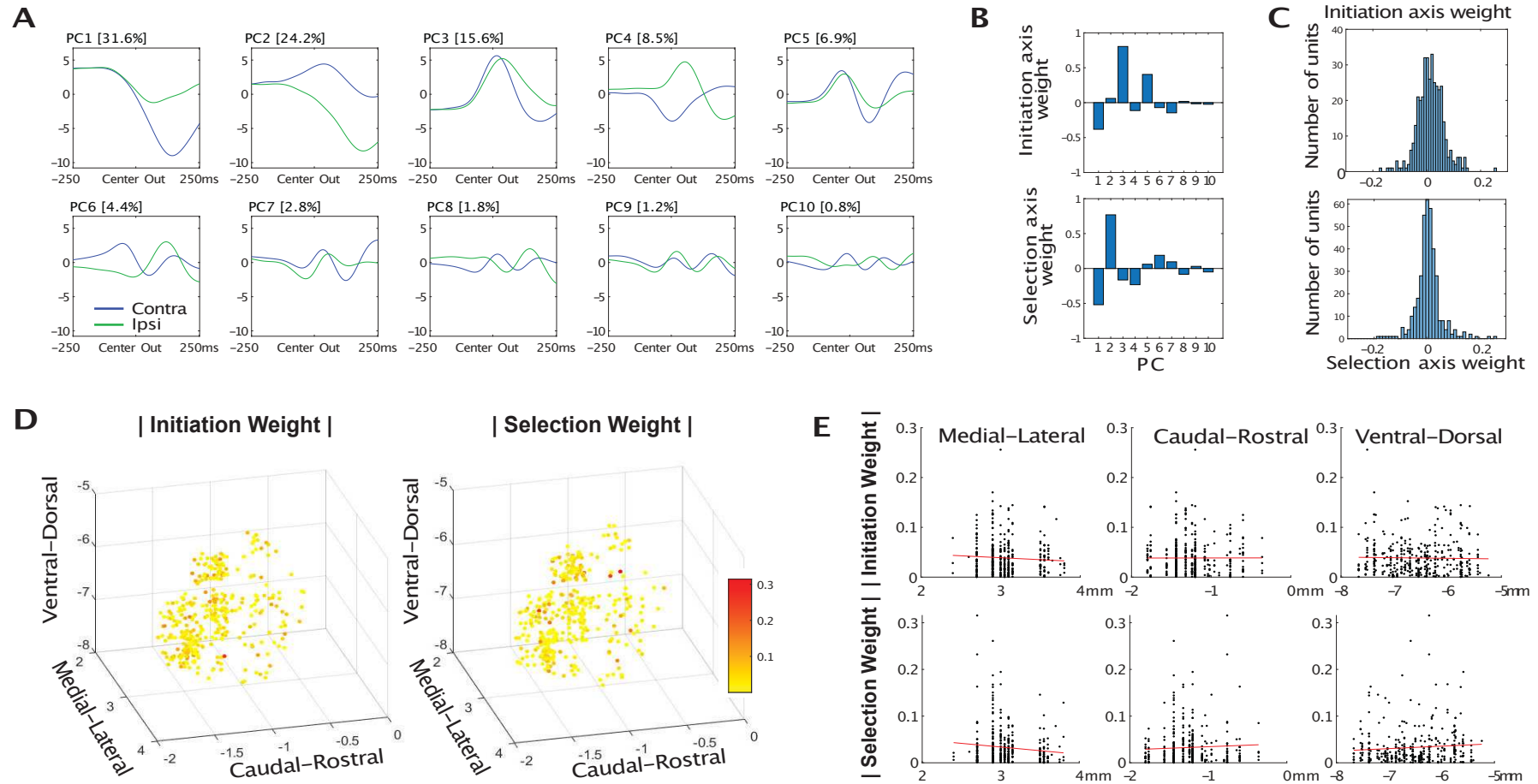
# Figure 3 - figure supplement 1



**Principal Components.**

**A**. The first 10 principal components.

**B**. Relative contributions of each PC to the Initiation and Selection Axes (i,e, the eigenvector of each Axis in the 10-PC space).

**C**. Weight of each GP neuron on the Initiation and Selection Axis.

**D,E.** Spatial arrangement of absolute weight values (positions in mm relative to bregma).

# Figure 4 - figure supplement 1
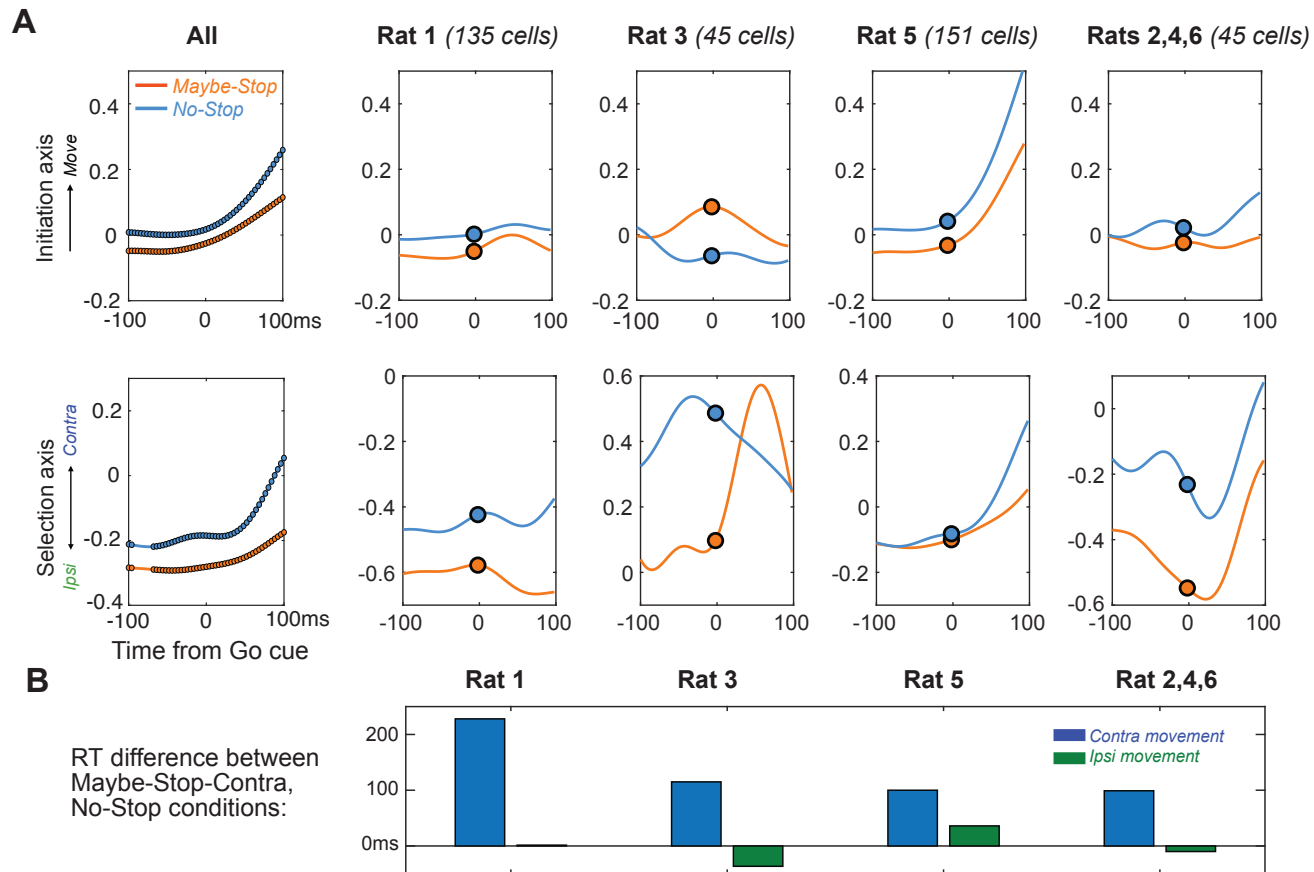


**Neural population results for individual rats, and corresponding behavior.**

**A.** Comparing proactive shifts along Initiation and Selection Axes for all rats together (left) and for individual rats. Rats 2,4 and 6 were grouped together as they had fewer recorded neurons. In all plots thicker lines indicate epochs of significant difference between two conditions (permutation test on each 4 ms time bin, p<0.05). Note that Rat 3 had the largest Selection Axis bias towards ipsiversive movements before the Go cue (and a bias *towards* movement on the Initiation Axis).

**B.** RT results for the same animal groupings. In all cases there was a greater slowing of contra than ipsi movements, consistent with a selective proactive inhibition effect. However, Rat 3 showed a *speeding* of ipsi movements compared to the No-Stop condition, consistent with an ipsiversive bias and no overall movement inhibition.

# Figure 4 - figure supplement 2

**Trial-history dependence.**

**A.** (Left) On Maybe-Stop trials that followed Stop trials ("After-Stop"), rats were more likely to succeed in stopping (Wilcoxon signed rank test, z=2.67, p=0.008) and showed increased RT (Wilcoxon signed rank test, z=4.46, p=8.02×10$^{-6}$), compared to trials that followed Go trials.
(Right) On No-Stop trials that followed error trials ("After-Error"), rats were more likely to make RT limit errors (Wilcoxon signed rank test, z=3.03, p=0.002) and showed increased RT (Wilcoxon signed rank test, z=5.42, p=5.95×10$^{-8}$).

**B.** Corresponding apparent shifts along the Initiation Axis did not reach significance (permutation tests, analysis epoch: -100 - 0ms before Go cue).
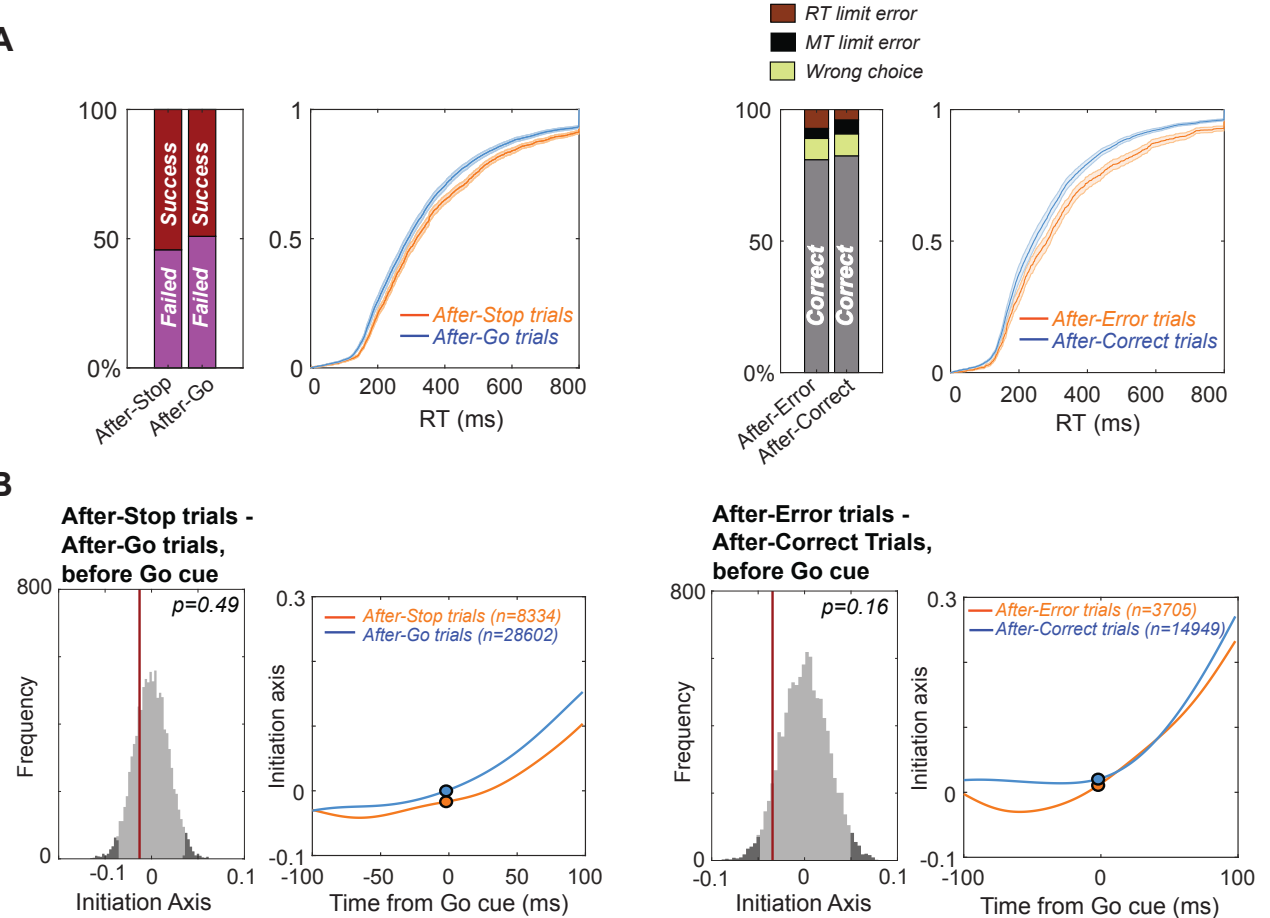
# Figure 5 - figure supplement 1

**Comparison of RT-matched Maybe-Stop and No-Stop trajectories.**

**A-C**, same as Fig. 5 A-C but using RT-matched subsets of trials. For RT matching, each RT from the Maybe-Stop condition was paired with the closest RT from the No-Stop condition; if no pair could be found within 250ms, the trial was not used. After RT matching the mean Maybe-Stop RT was 371ms (median 370ms) and the median No-Stop RT was 369ms (median 360ms).

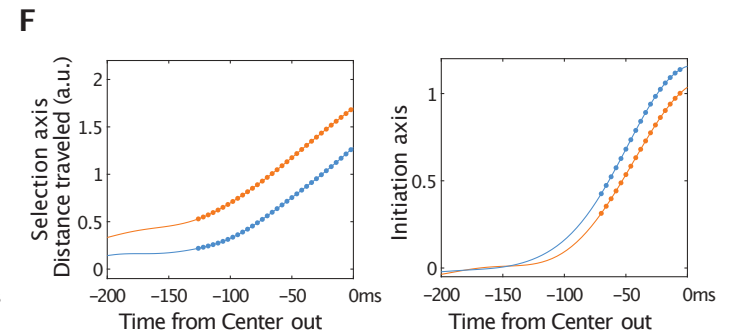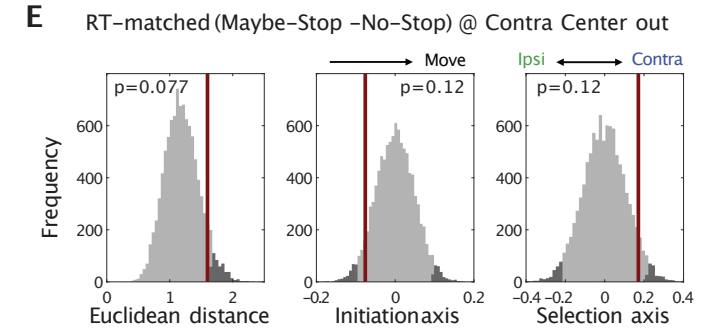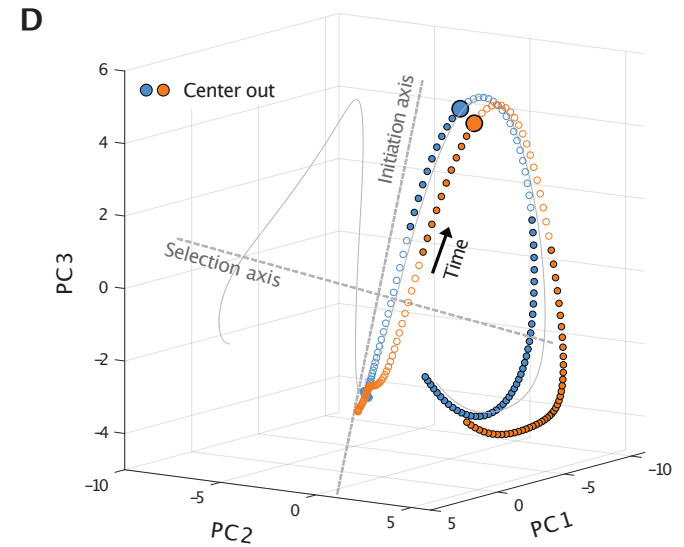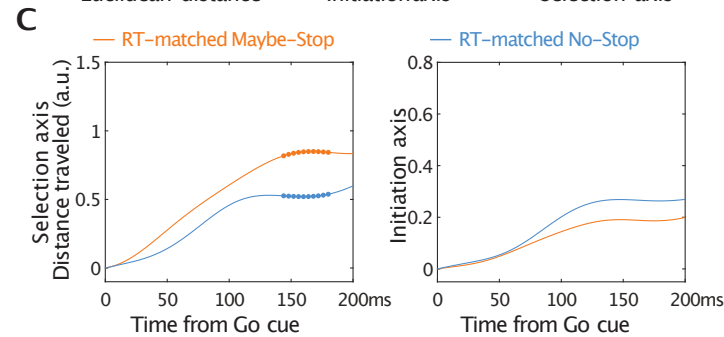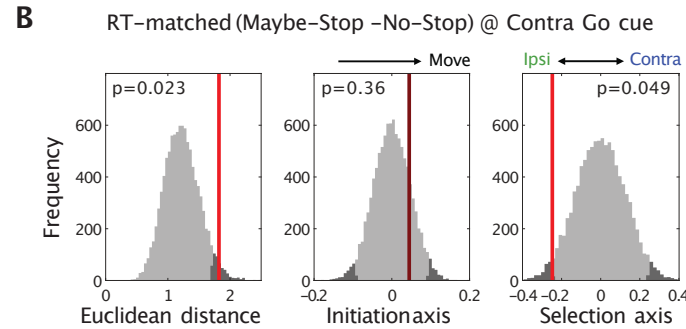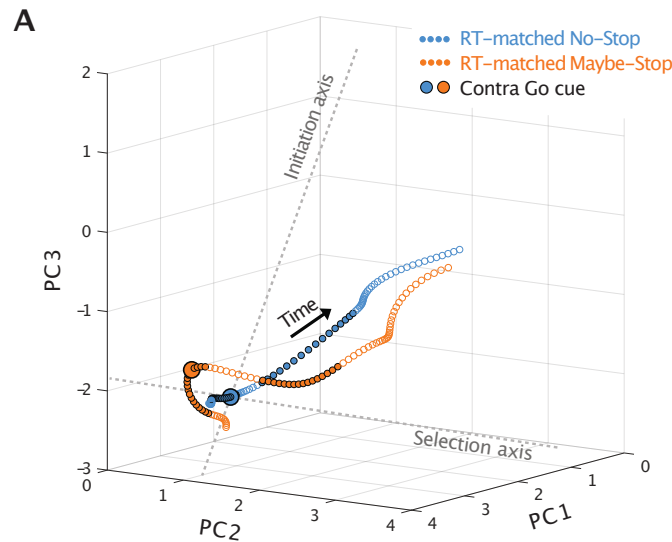**D-F**, same as A-C but aligned on movement onset (Center out).

# Figure 5 - figure supplement 2



**Comparison of Proactive and spontaneously Slow RT trajectories at movement onset.**

All panels are as Fig. 5, but aligned on movement onset (Center out).

**A**

No-Stop
Maybe-Stop
Center out

PC3

Initiation axis

Selection axis

Time

PC2

PC1

**B** Correct (Maybe-Stop – No-Stop) @ Contra Center out

p=0.0056

Move

Ipsi ←→ Contra

p=0.031

p=0.15

Frequency

Euclidean distance    Initiation axis    Selection axis

**C**

Maybe-Stop    No-Stop

Selection axis Distance traveled (a.u.)

Initiation axis

Time from Center out    Time from Center out

**D**

Slow RT
Fast RT
Center out

PC3

Initiation axis

Selection axis

Time

PC2

PC1

**E** Correct No-Stop(SlowRT – FastRT) @ Contra Center out

p=0.012

Move

Ipsi ←→ Contra

p=0.026

p=0.14

Frequency

Euclidean distance    Initiation axis    Selection axis

**F**

Fast RT    Slow RT

Selection axis Distance traveled (a.u.)

Initiation axis

Time from Center out    Time from Center out